Design and Analysis of Bow-tie Antennas for GPR Applications

Rashmiranjan Nayak

Department of Electronics and Communication Engineering
National Institute of Technology Rourkela

Design and Analysis of Bow-tie Antennas for GPR Applications

Thesis submitted in partial fulfillment

of the requirements of the degree of

Master of Technology

in

Electronics and Communication Engineering

specialization: Communication and Networks

by

Rashmiranjan Nayak

(Roll Number: 214EC5537)

based on research carried out

under the supervision of

Prof. Subrata Maiti

May, 2016

Department of Electronics and Communication Engineering

National Institute of Technology Rourkela

Department of Electronics and Communication Engineering
National Institute of Technology Rourkela

Prof. Subrata Maiti
Asst. Professor

May 31, 2016

Supervisor's Certificate

This is to certify that the work presented in the dissertation entitled *Design and Analysis of Bow-tie Antennas for GPR Applications* submitted by *Rashmiranjan Nayak*, Roll Number 214EC5537, is a record of original research carried out by him under my supervision and guidance in partial fulfillment of the requirements of the degree of *Master of Technology* in *Electronics and Communication Engineering*
specialization: Communication and Networks. Neither this thesis nor any part of it has been submitted earlier for any degree or diploma to any institute or university in India or abroad.

_____
Subrata Maiti

Dedication

Dedicated to my
beloved mother **Late Malati Nayak**,
father **Akshaya Kumar Nayak**,
younger brother **Jyotiranjan Nayak**,
sisters **Jyotirekha Nayak** and **Nibedita Swain**,
and niece **Stutee Sriya Sahoo**

Signature

Declaration of Originality

I, *Rashmiranjan Nayak*, Roll Number *214EC5537* hereby declare that this dissertation entitled *Design and Analysis of Bow-tie Antennas for GPR Applications* presents my original work carried out as a Postgraduate student of NIT Rourkela and, to the best of my knowledge, contains no material previously published or written by another person, nor any material presented by me for the award of any degree or diploma of NIT Rourkela or any other institution. Any contribution made to this research by others, with whom I have worked at NIT Rourkela or elsewhere, is explicitly acknowledged in the dissertation. Works of other authors cited in this dissertation have been duly acknowledged under the sections "Reference" or "Bibliography". I have also submitted my original research records to the scrutiny committee for evaluation of my dissertation.

I am fully aware that in case of any non-compliance detected in future, the Senate of NIT Rourkela may withdraw the degree awarded to me on the basis of the present dissertation.

May 31, 2016
NIT Rourkela

Rashmiranjan Nayak

Acknowledgment

With deep regards and profound respect, I avail this opportunity to express my deep sense of gratitude and indebtedness to Prof. Subrata Maiti, Department of Electronics and Communication Engineering, NIT Rourkela for his valuable guidance and support. I am deeply indebted for the valuable discussions at each phase of the project. I consider it my good fortune to have got an opportunity to work with such a wonderful person. I want to express my heartiest gratitude to Prof. K .K. Mohapatra, HOD, Department of ECE for his supports during my project work. I also want to express my sincere gratitude towards Prof. S. K. Behera for his constant motivation and suggestions during my tenure in NIT Rourkela. Sincere thanks to Prof. S. K. Patra, Prof. S. K. Das, Prof. S. Deshmukh, Prof. A. K. Swain. Prof. L. P. Roy and Prof. S. M. Hiremath for teaching me and for their constant feedbacks and encouragements. I would also like to thank all faculty members and staff of the Department of Electronics and Communication Engineering, NIT Rourkela for their generous help during my study period in the Institute.

I want to thanks to my friends, Chandra Shekhar Panda, Priyesh Prittam, Kapil Mangla, Debaprasard Mishra, Debaprasad Daxinray, Shasi Bhusan Jaiswal, Gyanedra Rout, Nihar Rajan Mohanty, Sunil Ghadei, Jnana Ranjan Sahu, Anam Das, etc. for their constant support and motivation during my study at NIT Rourkela. I would also want to say thanks my classmates Manasi, Narayana, Singdha, Rajesh, Karan, Manish, Gauttam and all other classmates for their generous help. I would like to take this opportunities to express my heartiest gratitude to Tanamaya Kumar Das, and Biswajit Dwivedy, Ph.D. Scholars of MAD laboratory of department of ECE; Sambit Kumar Mishra, Sampa Sahoo, Kshira Sagar Sahoo, etc. of Cloud Computing Laboratory of department of CSE for their unconditional support and motivation during my thesis preparation.

Last but not least I also convey my deepest gratitude to my mother Late Malati Nayak, and father Akshaya Kumar Nayak, family and relatives whose faith, patience and teaching have been always inspired me to walk upright in my life. Finally, I humbly bow my head with utmost gratitude before the God Almighty who always showed me a path to go and without whom I could not have done any of these.

May 27, 2016
NIT Rourkela

Rashmiranjan Nayak
Roll Number: 214EC5537

Abstract

Ground penetrating radar (GPR) is a non-destructive testing (NDT) technology, which uses electromagnetic (EM) techniques to map the buried structures in the shallow sub-surface. The efficiency of the GPR system significantly depends on the antenna performance as the signal has to propagate through lossy and inhomogeneous media. The GPR antennas should possess a low frequency of operation for more depth of penetration, ultra-wide band (UWB) performance for high resolution, high gain and efficiency for increasing the receiving power, minimal ringing, compact and lightweight for ease of GPR surveying. Bow-tie antennas are widely used as it can provide most of the above mentioned antenna performances. Though a number of researchers have carried out their research work for the design and development of the Bow-tie antennas for the GPR applications, still there is ample of scopes for the improvement of this antenna to achieve compactness and lightweight, reduced end-fire reflections, better gain and directivity, high radiation efficiency, etc. In this work, two improved Bow-tie antennas for the GPR applications have been proposed. A compact resistive loaded Bowtie antenna is designed and investigated which can provide an impedance bandwidth of 167% (0.4 - 4.5 GHz) with reduced end-fire reflections. The compactness is achieved by using a thin sheet of graphite for the resistive loading instead of using volumetric electromagnetic absorbing materials. The end-fire reflections are minimized by blending the sharp corners of the Bowtie antenna. However, the radiation efficiency and gain of the antenna are degraded significantly due to resistive loading which has been in the second proposed antenna by using an improved RC-loading scheme. The improved and compact RC-loaded Bowtie antenna with metamaterial based planar lens is designed and investigated which can operate over a UWB bandwidth of 3.71GHz (0.29 GHz - 4.5 GHz). This provides a maximum gain of 12.4 dB and maximum radiation efficiency of 94 % throughout the operating band. An improvement in the gain of 5 dB in the bore side direction is achieved by using a modified meta-material lens. The performance of both the designed antennas is investigated in the temperature varying environment and GPR scenario at the simulation level. A comparative analysis of the designed antennas with the other reported antennas indicates that the proposed antennas are advantageous for the GPR applications.

***Keywords*: *GPR*; *Resistive loading*; *RC-loading*; *Meta-material Lens*; *Bow-tie antenna*; *End-fire reflections*.**

Contents

List of Figures

List of Tables

Chapter 1

Introduction

The mankind is fascinated over centuries due to the possibility of detecting objects remotely without using a destructive testing method. There is a special radar technique which could probe the ground and its contents with high resolution and large depth of penetration. Hence, a considerable scientific and engineering effort has been utilized to gone into devising suitable methods of exploration. Ground penetrating radar (GPR) is a special type of radar technology, which is used to look into the ground to detect the buried target with high resolution and depth of penetration. Some popularly used synonyms for the GPR are ground-probing radar, sub-surface radar, surface-penetrating radar (SPR) , earth sensing radar and geo-radar [2, 7]. GPR can also be defined as a range of electromagnetic (EM) non-destructive testing (NDT) techniques primarily used to detect the location of interested object, i.e. target or various interfaces buried in the shallow sub-surface or located in a visually opaque medium such as concrete, rock structure, wall, etc. [7]. It finds a huge varieties of applications such as environmental applications, e.g. soil properties estimation, thickness, and properties estimations of snow, ice, and glaciers, contaminated land investigation, etc.; archeological applications, e.g. the NDT imaging technique to study the historical sites; civil engineering applications, e.g. borehole inspection, bridge deck analysis, building condition assessment, evaluation of reinforced concrete, pipes and cable detection, rail track and bed inspection, road condition survey, tunnel linings, wall condition, etc.; security applications, e.g. detection of buried mines (anti-personnel and anti-tank), etc. and geophysical investigations [2, 7, 8]. The basic principle of the GPR is based on the laws of reflection of the EM wave propagation. The GPR transmits the electromagnetic waves from its transmitting antenna to the ground or host media and receives the reflected signal generated due to the target and contrast in the material properties by the receiving antenna. The recorded data will be stored in the digital storage for further processing. The processing of these data through different signal processing schemes results in a good interpretation of the target and host media in terms of the structure of the object, depth of location, material properties of both the target and host media, etc. The EM signal propagation is highly dependent on frequency dependent behavior of the host media, i.e. soil, rock, etc. which are inherently lossy, inhomogeneous, and stochastic in nature. The material properties which

characterize the host media and the target are relative permittivity, relative permeability, and conductivity. However, conductivity and permittivity corresponding to the dielectric constant of the media, provides useful data for the GPR applications. The EM signal can penetrate very less in a highly conducting medium due to the rapid attenuation of the wave and hence depth of the penetration is controlled by the conductivity. The reflected wave is affected by the highly contrast nature of the dielectric medium which provides a good way to characterize the host media. The permeability will have a less significant impact on the EM wave propagation. The GPR is chosen to be more beneficial as compared to other NDT techniques used for the same application due to its high resolution and depth of penetration ability. However, low frequency of operation provides a more depth of penetration and low resolution. High frequency of operation corresponds to the ultra-wide band (UWB) performance provides high resolution with less depth of penetration. Therefore, always there is an optimistic trade off between required depth of penetration and resolution corresponding to the application. Hence, there is a requirement of an antenna which can operate in a low-frequency range with UWB performance so that a better depth of penetration and resolution can be achieved.

1.1 Motivation

The demand and applications of the GPR are rapidly growing in today's era due to the need of the NDT in various applications as mentioned in the previous section. GPR is one of the most popularly used NDT techniques due to its high depth of penetration, good resolution, low false alarm rate, low cost, less time consumption, ability to form three-dimensional images of the buried objects for ease of visualization and interpretation, etc. Hence, there is a huge demand of high-performance GPR system to meet the desired level of resolution and depth of penetration. The overall power efficiency of a GPR system significantly depends on the performance of the antennas used to transmit and receive radio frequency (RF) signal. A high performance GPR system needs an antenna which has characteristics of UWB, high gain, and efficiency, low operating frequency range, form factor, and proximity effect, etc. These are the major motivating factors which drives us to carry out our research in antenna design for the GPR applications.

1.2 Problem Statement

The major problems for the GPR systems are achieving good resolution, high depth of penetration, minimization of clutters, etc. To achieve high penetration depth, the GPR antenna to possess high radiation efficiency, better gain and directivity. The design and analysis of the GPR antenna is greatly differs from that of the antennas meant to communicate in the air or free space media. One has to take care of the extra precautions as GPR antenna

has to be operated with close proximity to the sub-surface media. The problem statement of this work can be outlined as follows.

- Achieving low frequency operation with out increasing its form factor.
- Difficulty of achieving UWB characteristics with typical fractional bandwidth exceeding 100%.
- Minimizing ringing effect with suitable design modification with out affecting other antenna performance parameters.
- Achieving dispersion less characteristics across a very wide bandwidth.
- Achieving low cost and modular antenna.

1.3 Objective

In this work, the two variants of the Bow-tie antennas are designed and investigated as the Bow-tie antenna can fulfill maximum of the stringent requirements of the GPR antennas. The major objectives of this thesis can be outlined as followings.

- To design an improved resistively loaded Bow-tie antenna having UWB performance and low frequency operation with high radiation efficiency.
- To design and investigate an improved RC (combination of resistive and capacitive) loading scheme to attain UWB performance and lower cutoff frequency.
- To increase the gain and directivity of the designed Bow-tie antennas significantly by using the Meta-material based planar lenses.
- To investigate the performance of the designed antennas in the temperature varying environment and GPR scenario.

1.4 Thesis Organization

In **Chapter 1**, introduction, motivation, problem statement, and objective of the thesis are presented in a nutshell. The organization for the rest portion of this thesis are briefly outlined as follows.

In **Chapter 2**, basics of GPR technology with various system parameters are elaborately presented. A comprehensive literature survey for the GPR antennas with emphasis on the Bow-tie antenna is presented. Various key features of the GPR antennas with major research challenges are addressed.

In **Chapter 3**, a compact resistive loaded Bow-tie antenna with reduced end-fire reflections is proposed. The compactness and minimal end-fire reflections are achieved with help of the improved loading scheme and suitable structural modifications.

In **Chapter 4**, an RC-loaded Bow-tie antenna with meta-material lens is proposed for the GPR applications. An efficient RC-loading scheme is proposed and investigated which can provide the UWB performance without decreasing the radiation efficiency significantly. Again, the gain and directivity of the antenna is improved with the help of a modified planar meta-material lens.

In **Chapter 5**, the overall conclusion of the thesis is briefly presented in terms of contribution and future scope.

Chapter 2

Background

2.1 Introduction

In this chapter, a brief background required for the basic level understanding of the Ground Penetrating Radar (GPR) technology and to carry out research for the design of antenna for the GPR applications are discussed. The chapter consists of three principal parts. A brief review of GPR technology is discussed in the first part. A brief review of the antenna candidatures for GPR applications is discussed in the second part. In the third part, a comprehensive literature review with recent trends of the antenna design methodologies used for the design of Bow-tie antenna is presented.

2.2 Brief review of GPR Technology

Ground penetrating radar (GPR) is a non-destructive testing (NDT) technology, which uses electromagnetic (EM) techniques to map the buried structures in the shallow sub-surface [7]. The GPR is also popularly known as surface penetrating radar (SPR) due to its ability to look into soils, walls, concrete structures, ice glaciers, etc.[7]. The literal meaning of GPR can be expressed as a radar technology meant to look the underground [8].Due to the rapid advancement in electronics integrated circuit (IC) technology and high end signal processing techniques, the GPR technology took a blow in the 1980s, which continues till today [2, 7, 8].

2.2.1 Basic principles of operation

The GPR transmits ultra-wideband (UWB) electromagnetic waves into the ground through an antenna. The reflected signals due to the contrasting nature of the buried targets and interfaces are received by the same antenna (monostatic mode of operation) or another antenna (bi-static mode of operation). These recorded data are stored in the digital storage device for the further processing to retrieve the vital information, i.e. depth, location and shape of the target. The processor determines the time duration taken by a pulse for the to and fro motion which is further used to determine the location of the buried object [7, 8].

The basic principles of GPR are almost same as that of ordinary Radar except the fact that the medium is soil, concrete, etc. instead of air or free space. Due to the heterogeneous and stochastic behavior of the ground, the GPR needs various extra precautions during system level design and signal processing. A simple diagram showing the basic principles of the GPR operating is shown in Figure 2.1.

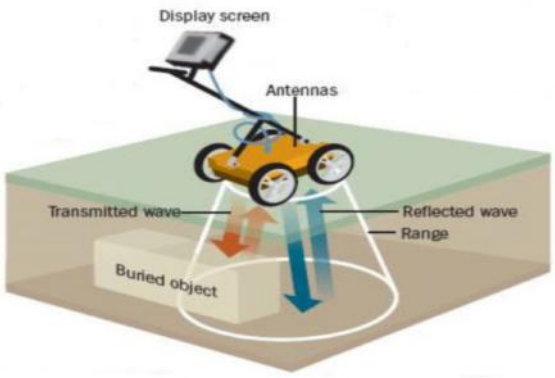

Figure 2.1: Typical GPR with basic principles [1]

2.2.2 GPR System

A generic block diagram of the GPR system is as shown in Figure 2.2. Broadly, the GPR system can be viewed as a Radar system consists of three major components, i.e. transmitter, receiver and central processing unit. The transmitter transmits EM signal into earth surface with the help of transmitting antenna. The receiver receives the reflected back energy with the help of receiving antenna. Then, this recorded data or signal undergoes various types of radio frequency (RF) signal processing techniques to map the location and structure of the buried object. The outputs of the processor can be displayed in the liquid crystal display (LCD) for the interpretation by the user. The EM contrasts due to change in dielectric permittivity ϵ, electric conductivity σ, and magnetic permeability μ results in the reflection, transmission and refraction of the EM waves. The recorded data can be classified into three types: A-scan (one dimensional data sheet) , B-scan (two dimensional data sheet) and C-scan (three dimensional data sheet) depending upon the scanning process through which the particular data is recorded during the GPR survey.

2.2.3 Classification of GPR Systems

Based on the domain of working and type of modulation scheme employed, the GPR systems can be classified as shown in Figure 2.3. Depending upon the domain of working, the GPR systems are classified as time domain GPR and frequency domain GPR. The time-domain GPR is also known as Impulse GPR . Further, depending upon the nature of modulation scheme used in the radar system, the time domain GPR systems are classified as amplitude

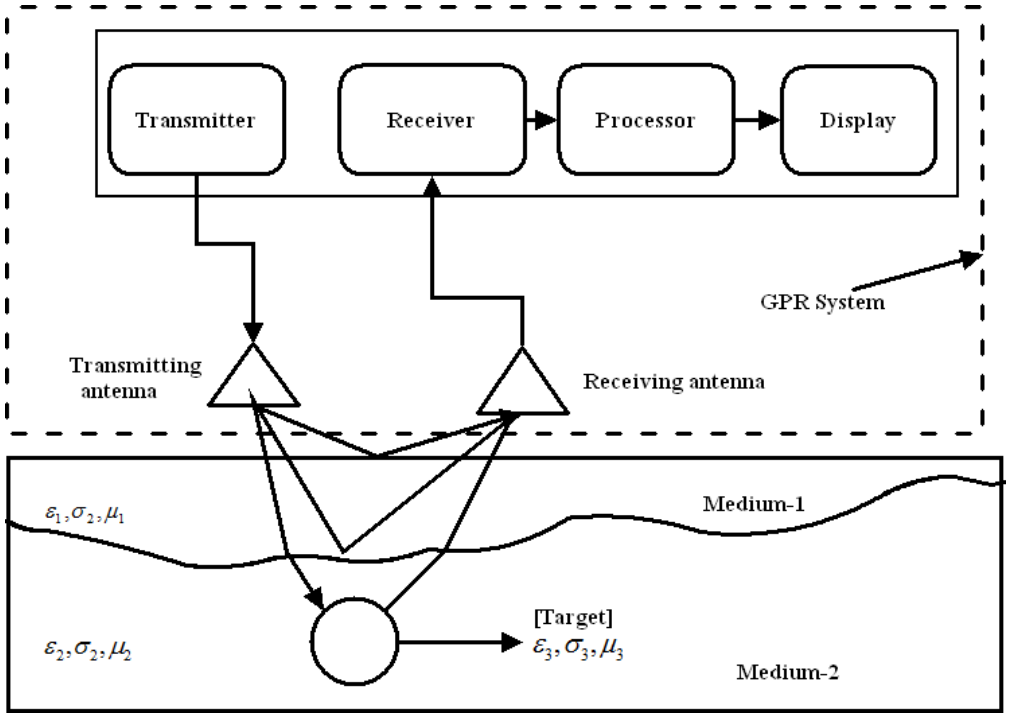

Figure 2.2: Generic block digram of the GPR system

modulated (monocycle) GPR and carrier free GPR. Similarly, the frequency domain GPR systems are classified as frequency modulated continuous wave (FMCW) GPR and stepped frequency GPR [9] .

1. Time-domain GPR (Impulse GPR)

This type of antenna is widely available in the commercial market. The time domain pulse of very short duration is transmitted and the reflected energy is received as a function of time. Range information can be determined based on travel time principle, i.e. time delay. The associated bandwidth is UWB in nature due to short pulse width. These short duration pulses, i.e. monocycle results in a good depth resolution [2, 9]. Advantages: ease of design and low-cost circuit [2, 9]. Disadvantages: Undesirable high ringing, resolution is limited by associated pulse width, a low value of duty cycle, inefficient use of transmitted power [2, 9].

2. Frequency domain GPR

Further, depending upon the pulse generation techniques, they are classified as following two categories.

(a) **Frequency Modulated Continuous Waveform (FMCW) GPR** : In this type of GPR, a continuous wave is transmitted at each frequency as the frequency synthesizer is varied continuously from one value to the other value. The range information can be

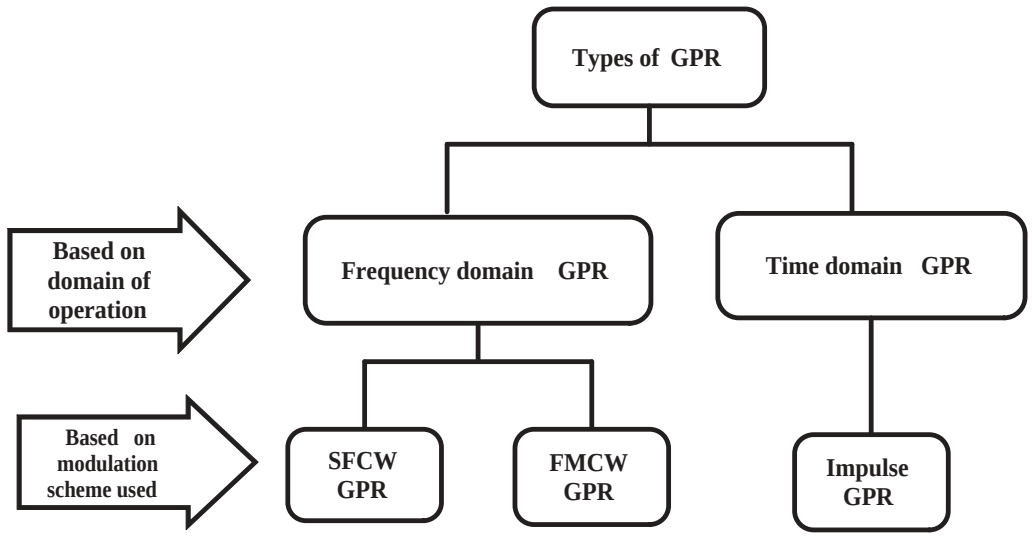

Figure 2.3: Classifications of the GPR systems [2]

found using the beat frequency [2, 9]. Advantages: Ease of design with low cost of implementation [2, 9]. Disadvantages: performance is degraded due to uncertainty in continuous frequency sweep [2, 9].

(b) **Stepped Frequency Continuous Waveform (SFCW) GPR** : In this type of GPR, the frequency synthesizer steps through a range of frequencies with equal steps. The amplitude and phase of the received signal are compared with the transmitted signal for each frequency. The recorded data in the frequency domain can be transformed into the time domain so as to produce the synthesized pulse with the help of inverse Fourier transformation [2, 9]. Advantages: More dynamic range, capable of using a narrow band coherent receiver, high SNR, transmission of frequency controlled energy, efficient use of power [2, 9]. Disadvantages: Complicated hardware, more acquisition makes the overall signal processing to be time-consuming [2, 9].

2.2.4 Governing Equations

Maxwell's equations can be rewritten for the GPR applications as follows [2, 7, 10].

$$-\nabla \times \mathbf{H} + (\sigma + j\omega\varepsilon)\,\mathbf{E} = -\mathbf{J} \tag{2.1}$$

$$\nabla \times \mathbf{E} + j\omega\mu\mathbf{H} = -\mathbf{K} \tag{2.2}$$

where **B** is electric field vector in V/m and **H** is magnetic field vector in A/m, **D** is electric flux density vector in C/m^2 , **B** is magnetic flux density vector in Tesla, **J** is current density vector in A/m^2 and ρ is charge density in C/m^3, ϵ is the dielectric permittivity which controls the velocity of the EM wave in a particular medium having dielectric constant ϵ_r and is given

by as follows.

$$v \cong \frac{c}{\sqrt{\varepsilon_r}} \tag{2.3}$$

The electric conductivity σ controls the attenuation of EM wave in a particular medium and μ is the magnetic permeability of the medium.

The propagation of the EM waves in the GPR scenario are primarily controlled by the propagation constant, reflection coefficient and transmission coefficient.The propagation constant is a complex quantity and consists of the attenuation constant α in Np/m as the real part and phase constant β in rad/m as the imaginary part as given below.

$$\gamma = \sqrt{-\omega^2 \mu \left(\varepsilon - j\frac{\sigma}{\omega}\right)} \tag{2.4}$$

$$\gamma = \alpha + j\beta \tag{2.5}$$

$$\begin{aligned} \alpha &= \sqrt{\tfrac{\omega^2\mu\varepsilon}{2}\left(\sqrt{1+\tan^2\delta}-1\right)} \\ \beta &= \sqrt{\tfrac{\omega^2\mu\varepsilon}{2}\left(\sqrt{1+\tan^2\delta}+1\right)} \end{aligned} \tag{2.6}$$

where $\tan\delta$ is the loss tangent and is given by

$$\tan\delta = \frac{\sigma}{\omega\varepsilon} \tag{2.7}$$

The wave velocity is given by

$$v = \frac{\omega}{\beta} \approx \frac{c}{\sqrt{\varepsilon_r}} \tag{2.8}$$

where c is the velocity of light in free space and ϵ_r is the relative permittivity of the medium defined as follows.

$$c = \frac{1}{\sqrt{\mu_0\varepsilon_0}} \tag{2.9}$$

$$\varepsilon_r = \frac{\varepsilon}{\varepsilon_0} \tag{2.10}$$

Reflection and transmission coefficients at a boundary: By applying boundary conditions, i.e. continuous tangential electric field and continuous normal magnetic fields, one can find the reflection coefficient Γ and transmission coefficient T as follows.

$$\Gamma = \frac{Z_2 - Z_1}{Z_2 + Z_1} = \frac{\gamma_1 - \gamma_2}{\gamma_1 + \gamma_2} \tag{2.11}$$

$$T = 1 + \Gamma = \frac{2Z_2}{Z_2 + Z_1} = \frac{2\gamma_1}{\gamma_1 + \gamma_2} \tag{2.12}$$

where Z_1 and Z_2 are the characteristics impedances of the medium-1 and medium-2

respectively; γ_1 and γ_2 are the propagation constants of the medium-1 and medium-2 respectively.

2.2.5 System Parameters of the GPR System

For the successful detection of the target by the GPR system in a practical scenario, it has to possess few important characteristics, i.e. high signal to clutter ratio, high signal to noise ratio (SNR), adequate spatial resolution of the target, and adequate depth resolution of the target [7]. There are different important parameters of the GPR system which primarily characterize and influence the system performance. These parameters are popularly known as system parameters of the GPR. To understand and implement the GPR system in practical applications, one has to familiar with these system parameters which are explained as follows.

(a) **Dynamic Range**: The dynamic range D_R can be defined as the ratio of largest receivable signal (Vmax) to the minimal detectable signal (Vmin) [2]. Mathematically, it is defined as in Equation 2.13. Usually, the D_R is expressed in decibels (dB) corresponding to a specific bandwidth. It is a vital parameter as it signifies the target detection ability of the GPR. It is desirable that the GPR should be able to handle a large energy signal reflected from surfaces and short range targets. Simultaneously, it should not miss the farther distanced targets or small target as a very less energetic signal near to the noise floor is received in this case. For the smooth operation of GPR, V_{max} (in Volts) must not overload the radar front end and V_{min} (in Volts) must be above the receiver noise level having a minimum detectable SNR [2]. Hence, the GPR should have high dynamic range.

$$D_R = 20 \log \left(\frac{V_{max}}{V_{min}} \right) \tag{2.13}$$

(b) **Bandwidth and frequency of operation** : Bandwidth and frequency of operation are two critical system parameters of the GPR system which determine the resolution and depth of penetration of the GPR respectively. The GPR will have better resolution only when the bandwidth of the antenna is very high, i.e. UWB and will have more depth of penetration only for the low frequency of operation. Thus, a set of frequency of operation and bandwidth can be selected for different applications of the GPR depending upon the desired resolution, and depth of penetration [9]. The operating frequency f_0 for the GPR is chosen corresponding to the desired depth of penetration by using Equation 2.14.

$$\log_e f_0 = -0.95 \log_e d + 6.15 \tag{2.14}$$

where where $d =$ depth of penetration in meter. Mathematically, the bandwidth BW can be defined as given in Equation 2.15 and 2.16.

$$BW = \frac{1}{\tau_p} \quad \text{for impulse GPR} \tag{2.15}$$

where τ_p is the duration of excitation pulse.

$$BW = f_{\max} - f_{\min} \quad \text{for CW GPR} \tag{2.16}$$

where f_{max} and f_{min} are the maximum and minimum frequency of operation for the CW GPR.

(c) **Resolution**: There are two types of resolutions used in GPR application, i.e. range resolution and lateral resolution. The power of the GPR to resolve between two closely spaced targets is known as range resolution or depth resolution. For GPR applications, two targets separated in time can be distinguished if the envelopes of their respective transient returns are clearly separated [2]. The depth resolution is defined in the following Equation 2.17.

$$R_{res} = \frac{(1.39)c}{2(BW)\sqrt{\varepsilon_r}} \tag{2.17}$$

where $c =$ speed of light, BW=bandwidth, and $\epsilon_r =$dielectric constant. When the resolution is measured in cross range direction, it is known as lateral resolution. Hence, to have better resolution, the GPR should have of UWB antenna, which means it should radiate very short pulses and narrow beam width in the operating bandwidth.

(d) **Unambiguous Range**:The largest distance at which a target can be detected without aliasing effect is known as unambiguous range R_{max} of the GPR. The unambiguous range of an impulse GPR primarily depends upon the programmable time window, i.e. pulse repetition interval T_r (PRI) and is given by Equation 2.18.

$$R_{unamb} = \frac{c.T_r}{2\sqrt{\varepsilon_r}} \tag{2.18}$$

The unambiguous range for the stepped frequency continuous wave (SFCW) GPR is primarily depend upon the bandwidth of operations (BW) and number of frequency steps (N). It is defined as in Equation 2.19.

$$R_{unamb} = \frac{N.c}{2(BW)\sqrt{\varepsilon_r}} \tag{2.19}$$

(e) **Power**:The GPR system can be operated with a variety of power sources, i.e.

rechargeable batteries and vehicle battery, etc. However, the GPR system should be designed in such a way that it will consume the power efficiently so that survey can be carried out for a longer duration without interruption.

(f) **Total Path Loss**:The range of the GPR system depends upon the total path loss which consists of three types of important losses, i.e. material loss, spreading loss and scattering loss (target reflection loss) [7]. Total path loss [7] is given in Equation 2.20.

$$L_{tot} = L_{eff} + L_{mis} + L_{trans1} + L_{trans2} + L_{spr} + L_{att} + L_{sca} \tag{2.20}$$

where, L_{eff} = antenna efficiency loss in dB, L_{mis}=antenna mismatch loss in dB, L_{trans1}= transmission loss from the air to the material in dB, L_{trans2}= Retransmission loss from the material to the air in dB, L_{spr}= Antenna's spreading loss in dB, L_{att}= attenuation loss of the material in dB, L_{sca}= Target scattering loss in dB.

2.2.6 Research Challenges in GPR

The basic principles of operation of the GPR system and conventional radar systems are same, i.e. both the systems are used to detect the target by using EM wave propagation principles. However, the GPR system is very much complicated due to the complex, heterogeneous and stochastic nature of the media to which it is applied. Though today the GPR system has advanced a lot and has been applied to numerous applications successfully, still it suffers from various challenges during the practical development and applications. The important research challenges for the GPR technology are as enlisted below.

(a) Estimation of media by accurate modelling of the GPR signal propagation in complex media such as soil, snow, etc.

(b) Modelling and design of antenna having UWB bandwidth and low frequency of operation which can be successfully operated within the near proximity to the ground.

(c) Detection of the buried target with low false alarm rate with efficient RF signal processing.

(d) Design of efficient shielding for the antenna to prevent the unnecessary picking off the other EM signals.

(e) Realization of the GPR system with low cost hardware.

(f) Ability to detect thin layered media.

(g) Achieving high scanning speed without slowing down the overall data acquisition process of the GPR system.

2.3 Antenna Technology for the GPR Applications

Antenna is a metallic device which is used to radiate and receive the radio waves. In other words, it act as a coupling device which couples energy from a source of radio frequency energy to a transmitting medium, i.e. normally air. All the important antenna performance parameters are indicated briefly as shown in Figure 2.4 as presented in [3]. It is also indicative that all the fundamental parameters exhibit frequency dependent behaviors.

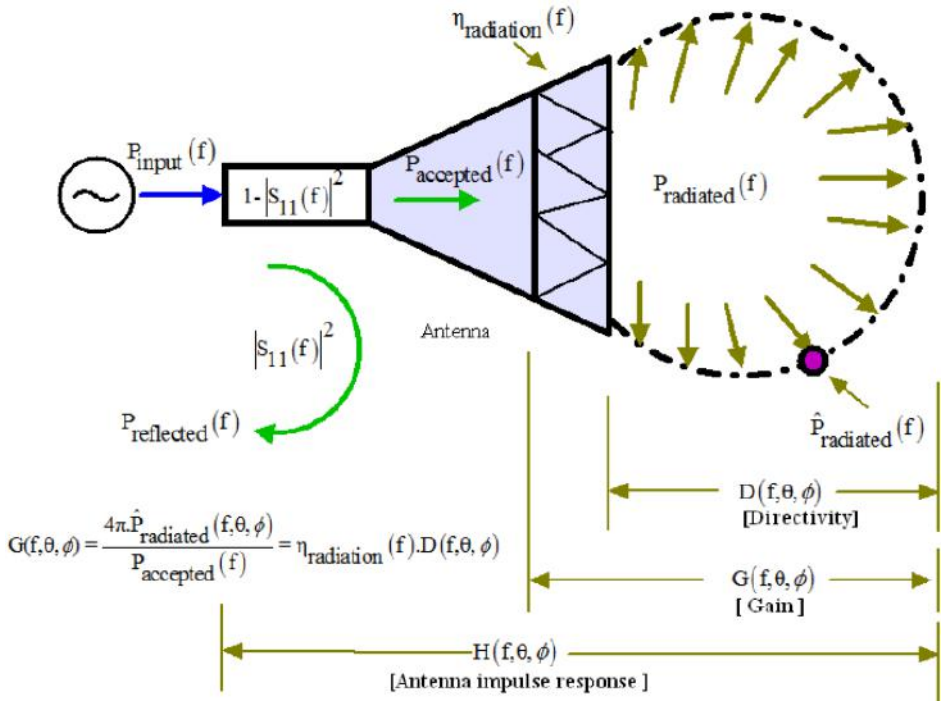

Figure 2.4: Basic performance parameters of a antenna [3]

As GPR antennas are operated in a very close proximity of the ground, its radiation characteristic changes significantly [2]. Hence, the modelling and design of antennas for the GPR applications are carried out with significant restrictions due to the nature of the media to which the antenna has to transmit the EM waves. It should take care of characteristics of propagation path, media through which EM wave will propagate, frequency at which GPR will operate to meet desired depth of penetration and bandwidth of operation to meet the desired resolution. Hence, generally the modelling and design of the antenna for GPR applications are meant to be application and medium specific. Usually, the propagation path or media, i.e. soil, concrete, mines area, etc. are lossy, inhomogeneous dielectric, occasionally anisotropic, stochastic in nature. Hence, these media act as low pass filter which puts restrictions on the upper frequency of the operation of the system. In other words, it can be said that the performance of the antenna is limited by the properties of the media [7].

Simultaneously achieving low frequency of operation for larger depth of penetration, UWB bandwidth for better resolution, and eliminating the impact of media on the upper cut-off frequency of the antenna are mutually conflicting tasks. So, it is always advisable to

model and design the antenna for GPR applications which will be corresponding to a desired range, resolution, and type of GPR system. Hence, the classes of the antenna which can meet this stringent demand are limited. The antennas are selected for GPR applications based on some important criteria: large fractional bandwidth, low time side lobes, low cross coupling levels, impact of the host media over the radiation pattern of the antenna [7].

Further, there is another set of criteria depending upon the type of GPR system which have to be fulfilled by the antenna so that it can be chosen as candidature for GPR applications. The antenna has to possess linear phase response, i.e. dispersion less characteristics so that it can be used in time domain (impulse) GPR system. This is required to avoid the complex receiver circuits consist of matched filter to deconvolve the effect of the frequency dependent characteristics of the antenna. However, for frequency modulated or synthesized GPR system, the need of linear phase characteristics can be relaxed by using appropriate system calibration process [2, 7].

2.3.1 Key features of GPR Antennas

The detailed explanations of the important features of the GPR antennas are explained in this section.

(a) UWB Bandwidth: A generic definition of UWB can be stated in terms of relative bandwidth [11] and is given by,

$$\left(\frac{2\left(f_h - f_l\right)}{\left(f_h + f_l\right)}\right) \gg 0.2 \tag{2.21}$$

where f_h and f_l are the upper and lower cutoff frequencies respectively. The standardized operating frequency range for the UWB are 3.1 GHz to 10.6 GHz (by U. S. FCC regulation) and 6 GHz to 8.5 GHz (by European regulation). However, there has been special allocations for the GPR applications [11].The antenna should radiate very short pulse and hence should possess UWB bandwidth which helps in achieving good resolution [12, 13].

(b) Low frequency of operation: The depth of penetration is inversely proportional to the frequency of the operation due to the frequency dependent behavior of the host medium. Hence, to achieve more depth of penetration, low frequency of operation characteristic should be possessed by the antenna [12, 13]. Hence, many times, the selection of the operating frequency of the antenna is an optimistic compromise between the physical size of the antenna and the penetration depth and resolution abilities of that antenna [14].

(c) High front to back ratio: The impact of the clutter , i.e. unwanted signals occurring in the same time window (or reflections from structures other than the target), should be

reduced significantly at the data acquisition level. This can be achieved by using an antenna having high front-to-back ratio [12, 13].

(d) High gain: When the frequency of the operation increased slightly more than 1GHz, the attenuation of the radiated pulse increases dramatically inside the host medium such as ground due to its frequency dependent nature. To minimize this effect of host media, the antenna should have possessed a good gain so that it amplitude of the reflected signal will be above the receiver noise level.

(e) High efficiency: The antenna should possess high radiation efficiency so as to increase the received power by overcoming the impact of the lossy host medium.

(f) Minimum ringing effect: The antenna should have a minimum ringing effect , so that the received pulse will be free of multiple oscillations having potentials to be treated as false alarm .

(g) Dispersion less characteristic : The antenna should have flat and constant amplitude response, and linear phase response with constant group delay so that it can be used in the impulse GPR systems. This is a vital criteria which prevents the distortions of the both transmitting and receiving pulses due to the inherent antenna nature. Hence, any distortions in the pulses can able to characterize the host media [2, 7, 12, 13, 15–17].

(h) Efficient EM Shielding: Usually, the GPR antenna operates in a close proximity of the ground so that a good amount of energy can be coupled to the ground and the reflected signals having a very small amplitude resulted from a distance located target can be received. However, there is a chance of reception of other existing RF signals such as GSM signal, Wi-Fi signal, etc. by the GPR antenna. Due to the superposition of the original target signal with these unwanted RF signals, sometimes the detection of the target can be missed out. Hence, there is a requirement of efficient shielding mechanism to protect the GPR antenna from such problems.

(i) High directivity: Usually, it is desired that the antenna should radiate maximum of its energy towards the host media, such as soil, concrete, etc. so that the overall efficiency of the GPR system can be enhanced greatly. To accomplish this, the GPR antenna should possess high directivity.

(j) Lowest transmitter and receiver antenna coupling: When GPR system is operated in bistatic mode , i.e. two different antennas are used to transmit and receive the EM waves, there is a possibility of direct coupling of the signal from transmitting antenna to the receiving antenna. This leads to increase in the overhead of receiving antenna, which indirectly mask the target. So, in this configuration, enough precaution should be taken to minimize the coupling between transmitting and receiving antenna.

(k) Compact size and lightweight: Maximum of the GPR applications involves field work, movable works, etc. For that reason, the GPR antenna should be compact and lightweight so that the overall size of GPR system reduces significantly. This also helps in ease of GPR surveying.

2.3.2 Antennas for GPR Applications

Only a few classes of antennas are considered as the potential candidates for the GPR applications due to stringent restrictions required for the GPR application as explained in the previous subsections. Hence, there are popularly used five common types of the antennas for GPR applications: dipole, horn antenna, Vivaldi antenna, bow-tie antenna and spiral antenna.

(i) Dipole

Dipole antenna is one of the elementary antenna which is successfully applied for the GPR applications. A typical dipole antenna is shown in Figure 2.5a. It is characterized by the linear polarization, low directivity and limited bandwidth. When an impulse is applied to the dipole, current and charge impulses will travel along the antenna length and at the end of the antenna endfire reflection will occur due to sudden discontinuity as shown in Figure 2.5b [7]. The problem of end fire reflection and limited bandwidth of the dipole can be decreased significantly by using resistive loading. The electric field component along E_z [7] is

$$E_z = -\frac{1}{4\pi\varepsilon_0}\int_{l_1}^{l_2}\left\{\frac{1}{c}\frac{dl}{dt} + \frac{dq}{dz|}\right\}\frac{1}{r}dz' \tag{2.22}$$

However, dipole antennas are unable to provide required bandwidth and gain for the satisfactory operation of the high-performance GPR [5]. Hence, dipole antennas are not used in commercially available GPR systems.

(ii) Vivaldi Antenna

Vivaldi antenna is one of the popularly used travelling wave planar antennas for the GPR applications. It provides high directivity and linear polarization which enables it for GPR applications [4]. It supports various modes of easy feeding mechanism such as microstripline, coplanar feedline, and direct symmetrical feeding. One of the popularly used taper profiles for Vivaldi antenna is exponential taper. The exponential taper is believed to be a priori wideband as it provides all the frequency components within the specified band with good radiation characteristics. One of the structures of the Vivaldi antenna is as shown in Figure 2.6. Vivaldi antennas can be resistive loaded by putting absorbing materials around

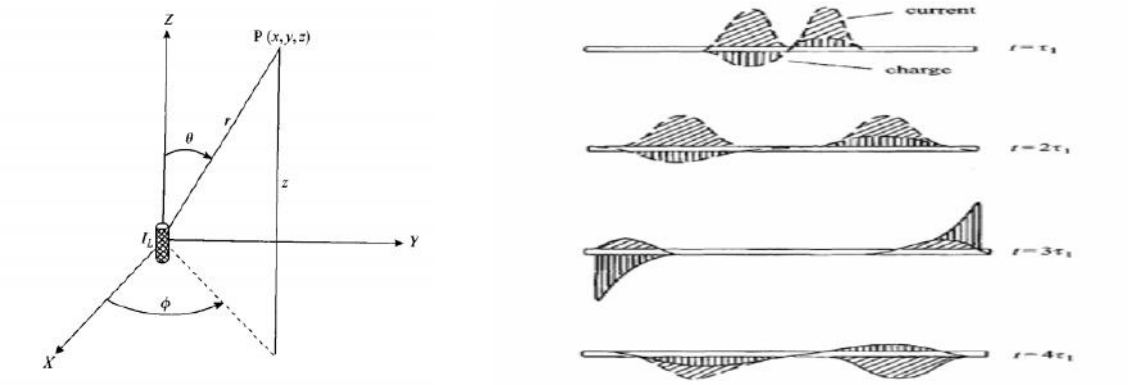

(a) Typical dipole antenna [7]

(b) Current and charge distribution of a dipole due to an applied impulse [7]

Figure 2.5: Dipole antenna and its end-fire reflection problem

the substrate edges. This helps to minimize the ringing effect without compromising on the transient response of the antenna [11].

Figure 2.6: Vivaldi antenna [4]

(iii) Planar Spiral Antenna

Planar spiral antenna is a frequency independent antenna whose structure is strictly defined by the angles. However, in practical applications, the antenna performance in the low frequency range is limited due to the truncation of infinite shapes into finite one [4]. It provides a circularly polarized wave with moderate amount of directivity and low front-to-back ratio. There are two widely used planar spiral antennas such as Archimedean spiral antenna and logarithmic spiral antenna depending upon the structure of the spiral. An Archimedean spiral antenna is as shown in Figure 2.7a [4]. Another logarithmic spiral antenna is as shown in in Figure 2.7b.These are not suitable for the time domain antennas as they suffers from ringing effect, i.e. long pulse dispersion.

(a) Archimedean spiral antenna [4]

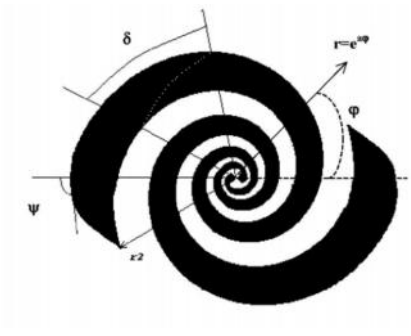

(b) Two-armed logarithmic spiral [5]

Figure 2.7: Planar spiral antennas

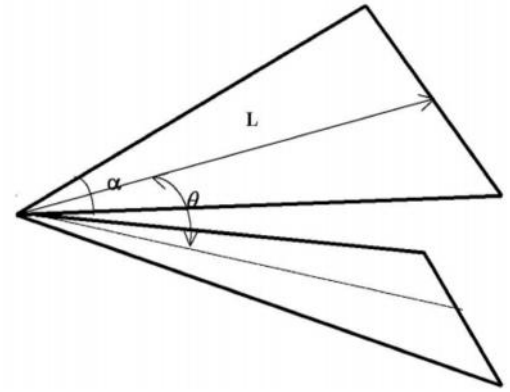

(a) 3-Dimensional TEM Horn geometry [5]

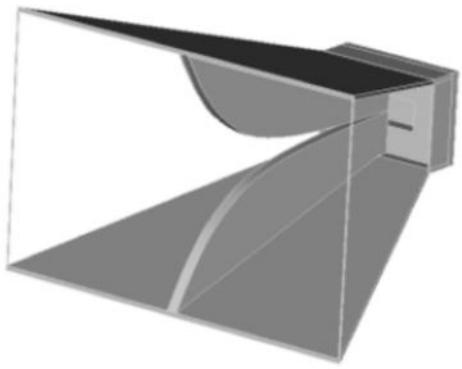

(b) 3-Dimensional TEM Horn geometry [4]

Figure 2.8: Geometries of TEM Horn antennas

(iv) TEM Horn Antenna

TEM Horn antennas are a special type of horn antennas capable of radiating TEM mode. It is more suitable for the time domain GPR system as it possesses UWB band, high gain, high directivity, narrow beam width, high front-to-back ratio as compared to the planar antennas used for GPR applications [5]. It is reported in [5] that the arm length of the TEM horn limits the lower cutoff frequency of the transmitted pulse, the plate angle indicates the polarization sensitivity and the plate elevation angle determines the structural impedance of the horn antenna. The bandwidth of the TEM horn can be significantly improved by using dielectric-filling techniques as it provides a gain behavior similar to the band pass filter. A basic geometry of TEM horn is shown in Figure 2.8a. Double ridge horn antenna (DRH) can be designed by inserting a pair of tapered metal ridges inside the horn which improves the bandwidth of the structure significantly [4, 18]. The geometry of a DRH is shown in Figure 2.8b. TEM horn antennas are not commercially used for GPR applications due to their large structure, heaviness and high price. Nevertheless, they are applied in the laboratory set up of the GPR as it is considered to be a standard reference antenna.

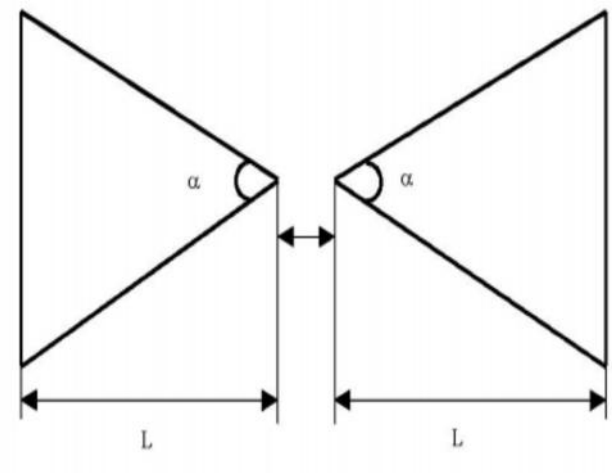

Figure 2.9: Basic triangular Bowtie antenna [5]

(v) Bow-tie Antenna

Bow-tie antenna is one of the element antennas which is a planar version of biconical antenna. One of the basic form of Bow-tie antenna is a triangular antenna as shown in Figure 2.9 [5]. The operation of Bow-tie antenna is similar to a dipole antenna. However, bow-tie antenna provide a good amount of directivity, efficiency and gain which enable it to be applied in GPR applications. This is one of the commercially popular GPR antennas due to its lightweight, compact and better antenna performances. It also suffers from endfire reflections similar to a dipole. However, the energy at the endfire reflections can be superimposed with the main radiating pulse in phase so as to give high efficiency [19]. The bandwidth of the Bow-tie antenna can be improved significantly by using restive loading. The Bow-tie antenna can be considered as one of the frequency independent antennas as its radiation pattern is expected to be independent of the frequency and its performance greatly depends upon the flaring angle α. A detailed literature survey regarding the operation, variations, design mythologies, etc. of the Bow-tie antenna is explained in the subsequent sections.

2.3.3 Comparative Analysis of GPR Antennas

Each class of the GPR antennas has certain antenna performance, which makes them suitable for a particular type of applications. However, a brief literature survey is carried to make a comparative analysis of the GPR antennas with respect to few critical antenna performance parameters as shown in Table 2.1 and Table 2.2.

From the comparative analysis, it is indicative that DRH antenna possesses the best antenna performances. However, it is not used popularly in the practical GPR application in the field due to its high design complexity, high price and large size. The Bow-tie antennas possess many attractive features such as planar and compact structure,ease of fabrication, low cost, high gain and directivity, etc. Therefore, it is chosen to investigate and design

Table 2.1: Comparative analysis of GPR antennas w.r.t. physical properties

Antenna type	**Structure**	**Overall Size**	**Design Complexity**
Dipole	3D, planar	small	low
Bow-tie	Planar, wire	medium	medium
Vivaldi	planar	medium	medium
Spiral	planar	medium	low
DRH	3D	large	high
TEM	3D	large	high

Table 2.2: Comparative analysis of GPR antennas w.r.t. radiation characteristics

Antenna type	**Rad. Pattern**	**Pol.**	**Gain (dB)**	**Dir. (dBi)**	**Eff. (%)**
Dipole	bidirectional	linear	low	low	low
Bow-tie	bidirectional	linear	moderate	moderate	moderate
Vivaldi	directional	linear	moderate	moderate	moderate
Spiral	bidirectional	circular	moderate	moderate	moderate
DRH	directional	linear	high	high	high
TEM	directional	linear	high	high	high

a novel class of Bow-tie antennas for GPR applications. The detailed further works are explained in the chapter-3 onwards.

2.3.4 Research challenges in the Design of GPR Antennas

Though a plenty of research is carried out to investigate and design various types of antennas for GPR applications, still there are ample of scopes for further investigation and design of antennas for the high performance GPR systems. Few of the important research challenges in the antenna design for GPR applications are enlisted as follows.

(a) To achieve UWB Bandwidth: Achieving UWB operation of an antenna, specifically towards the low frequency range, with approximately constant radiation pattern throughout the said band is a big problem in antenna design.

(b) To achieve low frequency of operation: Shifting of the frequency of operation towards a low frequency range without increasing the size of the antenna and decreasing radiation efficiency significantly is one of the major research challenges.

(c) To achieve high front to back ratio: Achieving high front-to-back ratio means complete suppression of one side lobes.

(d) To achieve High gain and directivity: To design of an antenna with high gain and directivity for GPR applications without compromising on the radiation efficiency.

(e) To achieve High efficiency: To obtain the UWB and ringing free performance of the antenna by the efficient loading schemes without compromising on the radiation

efficiency.

(f) To design efficient dispersion less UWB antenna: To design an efficient dispersion less antenna, i.e. antenna with flat amplitude response and linear phase response so as to obtain better performance of the Impulse GPR .

(g) To design an efficient and compact EM Shielding: There is demand for the design of lightweight, efficient, durable, and compact EM shielding for the GPR antennas.

(h) To achieve minimum transmitter and receiver antenna coupling: For the smooth operation of the GPR system in bistatic mode, both the antennas have to placed very close to each other with maximum isolation level so that their mutual effective radiation pattern will give better performance. Hence, there is a demand of proper mechanism or shielding which will isolate two antennas (transmitting and receiving antennas) completely.

(i) To design compact and lightweight GPR antenna: There is lots of scope in the design of compact and lightweight GPR antenna so that overall GPR system can be made to portable device.

2.4 Literature Review of the Bow-tie Antennas for the GPR Applications

The Bow-tie antenna is the planar version of bi-conical antenna. It is similar to dipole antenna, but with better antenna performance parameters such as gain, directivity, efficiency, linear polarization, etc. It is one of the most popularly used antenna for GPR applications due to its number of attractive features, i.e. light weight, ease of design and fabrication, better symmetry in radiation pattern, planar structure, compact size, low price, etc. Different variants of the Bow-tie antennas with enhanced antenna performances have been popularly used in the commercial GPR systems. These antennas have been used in maximum of GPR applications. In the section, a focused compressive literature survey related to the design and analysis of the Bow-tie antennas for GPR applications is carried out so as to grasp the recent trends in the antenna design methodologies.

There have been a number of research works carried out to either design a novel Bow-tie antenna or to enhance the antenna performance parameters of the existing antenna to make it suitable for GPR applications. Major research challenges involve in the design of the Bow-tie antennas with their design methodologies specific to GPR applications can be outlined as follows.

2.4.1 Low Frequency of Operation and Ultra Wide Bandwidth Characteristics

Antenna having the ability to operate in the low frequency range with ultra wide bandwidth (UWB) is always considered to be one of the best choices for the GPR applications. This is due to the reason that the antenna is capable of detecting targets buried at larger depth with high resolution. Hence, a lot of research work has been carried out to achieve low frequency of operation and wider bandwidth simultaneously by the Bow-tie antenna. Design of the Bow-tie antenna operating in low frequency with UWB and compact size for the GPR applications is one of the major research challenges for the research community. This is achieved by mainly use of various ways of embedded loading techniques and structural modification techniques applied to the Bow-tie antenna as discussed below.

(a) Structural modification techniques

Many researchers have been trying to achieve UWB performance of the Bow-tie antenna by using various structural modifications of the Bow-tie antenna. Different bandwidth enhancement techniques such as use of multi-stage twin feed lines, tapered slot, round or staircase Bow-tie antennas have been used to achieve UWB performance [13]. A self-complementary principle was applied to planar Bow-tie antenna with fractal structure to achieve UWB performance from 2.8 GHz to 10.5 GHz as reported in [20]. Two triangular patches are printed on either side of the substrate to achieve the self-complementary structure. However, due to the absence of the lower frequency operation and presence of monopoles like radiation pattern disqualifies it for the GPR applications, though it is very much suitable for the other applications. A double sided Bow-tie antenna is also capable of achieving UWB performance due to its truncated ground plane and tapered feed line as reported in [13]. The bandwidth of a double side printed Bowtie antenna can be improved significantly by overlapping its two arms as reported in [21, 22]. The bandwidth of the Bowtie antenna is significantly improved with introduction of the slots, stubs in the antenna geometry as reported in [23]. Nevertheless, all these structural adjustments are able to increase the bandwidth to achieve the UWB performance are applied solely to the high frequency range and can't be given to achieve UWB by lowering the lower cutoff frequency in the MHz range. Hence, it is indicative that only structural modifications can't be applied to the Bow-tie antenna with compact size to achieve UWB performance for the GPR applications. From literatures, it is also figured out that structural modification of the Bow-tie antenna is always accompanied by any one of the loading techniques to achieve UWB performance so that it can be suitable for the GPR applications.

(b) Resistive loading techniques

Special efforts are taken to reduce the lower cutoff frequency with the help of resistive loading so that higher depth of penetration can be achieved. Similar to the dipole antenna, the bow-tie antenna also suffers from ringing effect as discussed in chapter 2. Late time ringing phenomena which are potentially responsible for the masking of buried targets in a GPR survey can be prevented by using resistive loading technique [24]. When current flows from feed line to the either sides of the Bow-tie arms, it should gradually decrease so as to minimize the high reflections resulting from the distant sides of the Bow-tie arms. This can be achieved by using suitable restive loading profile. Restive loading antennas are preferred for the GPR applications due to its ability to radiate very short pulses, provide UWB, and suppress late-time ringing [12]. A very widely used resistive loading profile known as Wu-King resistive loading profile was successfully proposed and implemented for a monopole antenna as reported in [25]. The Wu-King resistive profile provides a continuous smooth variation of resistances across the antenna length and is a function of the antenna length and antenna input impedance at the feeding point. The Wu-king profile can be expressed as follows [25].

$$z^i\left(z/h\right) = \frac{\varsigma_0 \psi}{2\pi h\left(1-\frac{z}{h}\right)} \tag{2.23}$$

where z/h is the relative distance along the monopole from the coaxial aperture,$\zeta_0 = \sqrt{\mu_0/\varepsilon_0}$ and ψ is a dimensionless parameter derived for the current distribution for the antenna. A modified Wu-King profile was applied to a resistively loaded Vee dipole to achieve reduced reflection from the drive point of the antenna and increased forward gain as reported in [26]. A pair of UWB transmit/receive antennas with low cross coupling were developed with resistive loading using Wu and King profile which is suitable for the impulse radar as reported in [27]. However, Lestari, et. al. had been working on resistive loaded Bow-tie antenna for the GPR applications as reported in [28–30]. As reported in [28], a compact UWB Bow-tie antenna was designed using resistive loading with an improved loading profile so as to minimize the late-time ringing. Here, lumped resistors are arranged so as to follow the loading profile across the antenna in such a way that loading increases from the feed line to the either sides of the Bow-tie antenna. By using shielding, they had increased the directivity of the antenna. However, the frequency domain analysis is missing in this work. Again, in [29]. Another improved Bow-tie antenna for GPR applications with an efficient pulse radiation capacity was reported. Here, along with the lumped resistor loading, a bending of the planar version of the wire Bow-tie antenna is introduced between feed point and the distant edge of the arms so as to constructively superimpose the main pulse with the secondary pulse. This results in the high efficient pulse radiation, which makes the antenna more suitable for the commercially available impulse GPR. The distance between

the feed point and bending location is given by in Equation 2.24.

$$d_{bend} = \frac{c}{4f_c\sqrt{\varepsilon_r}} \tag{2.24}$$

where c is the speed of light, f_c central frequency of the excitation pulse and ε_r is the relative permittivity of the substrate. Recently, a modified Bow-tie antenna with ability to radiate improved pulse is reported in [30]. Here, the secondary radiations introduced by the resistive loading are used to increase the amplitude of the pulse significantly. An analytical expression for an improved loading profile for the GPR antenna capable of providing better input impedance bandwidth, efficiency and reduction in ringing was reported in [31]. In [32], a special type of resistive loaded Bow-tie antenna using Genetic Algorithm (GA) was developed with the help of lumped resistors mounted on the planar strips of the Bow-tie antenna for the application of Breast cancer detection. A lumped resistor loaded Bow-tie antenna covered by a rectangular cavity having inner walls coated partially or fully with ferrite absorber was reported in [33]. The main contribution in this work was an improvement of the impedance characteristics of the GPR with the help of ferrite coated inner walls present in shielding box. A good and in-depth analysis of the resistor loaded Bow-tie antenna for the GPR applications was presented in [34]. The antenna performance depends mainly on the total parallel end-resistors and is independent of the number of resistors used. The corners of the Bow-tie arms are the best position to place the resistors. Thought the resistive loading is capable of bringing the lower cutoff frequency to a lower frequency range while providing UWB performance, it degrades the antenna radiation efficiency significantly. Hence, many researchers have been trying to implement other form of loadings as discussed in the subsequent sections.

(c) Capacitive loading technique

The major disadvantages of the resistive loading is reduction in radiation efficiency which can be significantly minimized by using capacitive loading. Capacitive loading with the introduction of azimuthal slots in the Bow-tie antenna was realized as reported in [35]. In this scheme, the bandwidth of the antenna is increased significantly with reduced ringing effect without decreasing the radiation efficiency significantly. A slotted Bow-tie antenna with increased bandwidth is also realized with help of azimuthal slot on the antenna was presented in [36]. This slot acts as an RC-loading scheme. However, only capacitive loading though capable of increasing the bandwidth, but unable to remove the ringing effect significantly.

(d) RC loading technique

A RC-loaded cylindrical antenna with broadband behavior was reported in [37]. An analytical analysis of the RC loading profile which can be used for enhancement of the

antenna bandwidth was presented in [38]. An UWB Bowtie antenna having a good transient behavior resulted from RC-loading scheme and can be used for the time domain GPR systems was reported in [39]. A loading scheme consists of both restive and capacitive loading applied to the Bow-tie antenna so as to produce improved pulse radiation is reported in [40]. Here, the constant resistive loading is realized by volumetric microwave absorbers. A linear capacitive loading is realized with help of number of narrow concentric slots present on the antenna surface. The slot close to the feed point is utilized as a secondary source of radiation. However, this antenna was bulky and the frequency domain behaviors were not discussed. Recently, a modified RC-loading scheme along with some meta-material lens applied to the Bow-tie antenna has been proposed in [6, 12]. This antenna is capable of providing UWB performance with high gain and front to back ratio which makes it more suitable for the GPR applications. However, there is a requirement of more research to increase further the bandwidth and efficiency of the Bow-tie antenna with the help of new scheme of RC-loading.

(e) RL loading technique

A lumped resistor-inductance loading, i.e. RL loading has been proposed in [41] which is capable of bringing the operating frequency to a low frequency of 0-300 MHz without decreasing the radiation efficiency. But, it suffers from low bandwidth. A dielectric horn fed Bow-tie antenna for the GPR applications was proposed in [42]. But, it has complex geometry with comparably less bandwidth.

(f) Cavity backing technique

Many research works have proposed that, the increase in the bandwidth of the Bow-tie antenna by lowering the lower cutoff frequency can be achieved by making the antenna cavity-backed. The backed cavity made up of volumetric absorbing materials act as the resistive loading which decrease the lower cutoff frequency to increase the bandwidth and also capable of increasing the directivity and front-to back ratio when it is covered with a proper shielding. A variety of schemes for the realization of backing cavity can be found in [24, 43–45] where cavity filled with different layers of EM absorbing materials are used to achieve UWB by lowering the lower cutoff frequency. A good analysis of lumped resistor loaded half-ellipse bow-tie antennas with backed cavity was reported in [46]. Here, backed cavity is used to increase the bandwidth and directivity. F. Sagnard, et al. proposed various types of coplanar waveguide fed slot Bow-tie antenna with cavity backed structures for the GPR applications as reported in [47, 48].However, the design and availability of the volumetric EM absorbers matching exactly to the required loading profile is one of the research challenges. Due to cavity backed structure, the overall size and weight of the antenna also increases. Hence, there is requirement of compact, lightweight and efficient, backed cavity scheme for the GPR antennas.

2.4.2 High Gain and Directivity

The antenna of surface penetrating radar (SPR) many times used at a close proximity of host media, i.e. soil, concrete, etc. so as to transfer more energy to the media. But, the low pass filter behavior of the ground restricts the antenna to achieve it. Therefore, many researchers have been tried in a number of ways to achieve more coupling of EM signal to the ground media by enhancing directivity and gain of the Bow-tie antenna. The directivity and front-to-back (F/B) ratio of a compact Bow-tie antenna is increased significantly by using planar reflector behind the antenna as reported in [49]. The directivity of a partially lumped resistor loaded Bow-tie antenna is increased with the help of trapezoidal cavity as reported in [50]. Due to cavity structure the overall size of the antenna also increases. Meta-material lens are also used to increase the gain and directivity of the Bow-tie antenna a reported in [6, 12]. However, there this limits the bandwidth of the antenna in both lower frequencies due to difficulty of designing meta-material in low frequency range. Hence, there is requirement of the Bow-tie antenna having high gain and directivity with compact and less complex structure.

2.4.3 Achieving High Radiation Efficiency

GPR systems are generally used in field works and they draw power from the portable batteries. The power consumption by the processor of the GPR system are decreased significantly due to significant growth in low power VLSI (very large-scale integration) systems. So, the majority of the power is utilized by the antenna part of the GPR system. This results in high cost and more time consuming for the GPR survey. Hence, many researchers have tried to prevent wastage of power by designing the Bow-tie antennas with high radiation efficiency. The radiation efficiency of the Bow-tie antenna can be significantly increased by making the corners of the Bow-tie arm as rounded structures as reported in [51] and it also helps in increase in bandwidth. The radiation of the Bow-tie antenna is mainly due to the superposition of the direct radiations from the feed (or main pulse) and strong diffractions (or end reflections or end-fire reflections) from the two ends of the Bow-tie arms as reported in [19]. The reduction in end reflections results in higher radiation efficiency.

2.4.4 Compactness and Lightweight

As many applications such as inspection of railway track, road, etc. are carried out at remote locations or fields, the overall size and weight of the GPR system should be less. The major portion of the weight and size of the GPR system is due to antenna only. Hence, many researchers have tried in numerous ways to make the Bow-tie antenna more compact and lightweight so that it will be more suitable for the GPR applications. A small flexible Bow-tie antenna was reported in [52], but it has a very narrow bandwidth. Many research works have

been carried out to make the Bow-tie antenna compact by using various configurations, still the low frequency of operation with UWB performance is the major constraints towards this goal. Hence, there is a requirement of more focused research in this area.

2.4.5 Achieving Stable Radiation Pattern over Wide Bandwidth

The GPR antenna operates over a wider bandwidth so as to achieve high resolution. From this, the antenna should radiate in the same manner over a wide frequency range. It is possible only when the radiation pattern remains almost same throughout the said band. Hence, a lot of research work has been carried out to achieve a stable radiation pattern of the Bow-tie antenna over a wide band. Various ways to maintain the stable radiation pattern of the Bow-tie antennas with help of different geometries of the cavity structures are presented in [53–56]. However, the design and fabrication process of these antennas are very complex and their size is also large. Hence, there is need of technique through which stable radiation pattern can be achieved with compact and simple geometry of the antenna.

2.4.6 Achieving Frequency Reconfigurability

Selection of the frequency of operation and bandwidth of the antenna has been always application specific. So, one antenna suitable for a particular application, e.g. detection of mines may not be suitable for another application, e.g. quality inspection of plaster of the cement wall. It has been always a burden in terms of cost, portability, and feasibility for the user who wants to use the GPR system for multiple applications. Hence, there is a demand of frequency reconfigurable antenna which can change its operating frequency depending upon the requirement in accordance with the applications. Few researchers also attempted to explore this frequency reconfiguration behavior of the Bow-tie antenna. A reconfigurative approach is used for stepped frequency GPR prospecting which involves placing of two GPR antennas in different orientations [57]. However, it deals with experimental works. A reconfigurable Bow-tie antenna was reported in [58]. It uses geometry morphing approach which is a most structurally complicated method used to achieve reconfigurability of the antenna. But, it provides a very narrow impedance bandwidth. Achieving frequency reconfigurability over a UWB range is one of the most difficult task for the antenna designers.

2.5 Summary

The GPR is found to be more popular among the other NDT schemes due to its high resolution and depth of penetration. The antenna is a critical component of the GPR system whose performance can significantly affect the overall system performance. Due to various stringent requirements by the GPR system, only few antennas such as Hon antenna, Bow-tie antenna, etc. are eligible for the GPR applications. Bow-tie antenna is popularly used for

the GPR applications due to its various attractive features such as planar structure, low cost, lightweight, high gain and directivity, etc. Based on the comprehensive literature survey and comparative analysis of the GPR antennas, it is noticed that there is a requirement of compact, low cost, and UWB bow-tie antenna for the GPR applications. The compactness of the antenna is highly essential for the GPR applications so as to achieve ease of GPR surveying. Various loading schemes such as R-loading, RC-loading, etc. can be used to attain the UWB and ringing free performance of the antenna. However, there is requirement of improved loading scheme which can provide the UWB and ringing free performance specifically in the low-frequency range without decreasing the radiation efficiency significantly. Though number of research works have tried to improve the Bow-tie antenna performance to make it suitable for GPR applications, there are ample of scopes to improve the Bow-tie antenna with respect to compactness, high efficiency, reduced end-fire reflections, high gain, high directivity, etc.

Hence, this chapter can be considered as a fundamental backbone for our research work related to the development of the Bow-tie antennas for the GPR applications which are presented in the subsequent Chapters.

Chapter 3

Design of Resistive Loaded Bow-tie Antenna with Reduced End-fire Reflections

3.1 Introduction

There is a huge demand of the compact Bow-tie antenna having UWB and ringing free performance for the GPR applications due to its ability of providing high resolution and depth of penetration with more accuracy. Many works have been focused to obtain UWB performance by lowering the lower cutoff frequency with the help of resistive loading. However, these schemes provides the UWB performance at the cost of radiation efficiency and large size of the antenna due to use of volumetric EM absorbing materials. The decrease in the radiation efficiency is mainly due to the end-fire reflection, i.e. reflections occurring at the either sides of the Bow-tie antenna due to the sharp corners of the antenna structure. Hence, there is requirement of compact, UWB, Bow-tie antenna with minimal end-fire reflections.

The rest of the chapter is organized in the following manner. The related works to the resistively loaded Bow-tie antennas are briefly presented in the Section 3.2. A basic theoretical analysis with design equations are discussed in the Section 3.3. The section 3.4 explains the detailed design methodologies of the proposed antenna. The simulated and measured results are discussed in the section 3.5. Investigation on antenna performance due to the temperature variations both inside the antenna body and its surroundings is carried out with help of thermal and mechanical co-simulation in multi-physics environment of CST Microwave studio v.15 as discussed in the section 3.6. To study the performance of the proposed antenna in the GPR environment, it is simulated in the GPR scenario implemented Computer simulation technology (CST) Microwave studio v.15 as discussed in section 3.7. Comparative analysis of the antenna is presented in section 3.8 followed by conclusion in 3.9.

3.2 Related Work

Different variants of Bow-tie antenna with improved antenna performances i.e. gain, efficiency, bandwidth, etc. have been proposed for GPR applications in [12, 13, 19, 24, 46–48, 51]. Special efforts such as loading techniques are taken to reduce the lower cutoff frequency so that higher depth of penetration can be achieved [12, 24, 48]. A double sided Bow-tie structure printed on dielectric substrate where truncation of the ground plane is used to achieve UWB from 3.1 GHz to 10.6 GHz [13]. The efficiency of the Bow-tie antenna can be improved significantly by utilizing the energy in end-fire reflections if the antenna is excited by the bipolar pulse [19]. The bandwidth of the Bow-tie antenna can be enhanced to achieve UWB performance by using different bandwidth enhancement techniques such as using tapered slot, multi-stage twin feed lines, round or stair case Bow-tie antenna structures [13], Coplanar waveguide feed lines [51], using triangular monopoles with rounded corners [51], loading stubs and using annular ring load [19], etc. The resistively loaded Bow-tie antenna is preferred for the GPR applications as it can radiate very short pulses and provides UWB [12], suppresses late-time ringing [19]. However, due to embedded loading and resistive loading, the lowest operating frequency and antenna impulse response can be slightly affected at different operative conditions [24]. The radiation of a Bow-tie antenna is mainly due to the superposition of the direct radiations from the feed (or main pulse) and the strong diffractions from the two ends (or end reflections) [19]. Though number of research works have tried to improve the Bow-tie antenna performance to make it suitable for GPR applications, there are ample scopes to improve the Bow-tie antenna with respect to compactness, high efficiency, reduced end-fire reflections etc.

3.3 Theoretical Analysis of Bow-tie Antenna

Triangular Bow-tie antenna (TBA) is considered as one of the basic configuration of the Bow-tie antenna. A typical structure of a triangular Bow-tie antenna with relevant physical parameters is shown in Figure 3.1. It is also considered as one of the frequency independent antenna whose performance mainly depends upon the flare angle instead of the width and length of the antenna. The basic geometry of the Bow-tie antenna is determined by three parameters [19] i.e. flare angle θ_0 which mainly affects the bandwidth, gap distance g which can slightly influence the antenna performance, arm length a which is closely related to radiation efficiency. A brief theoretical analysis required for the design and analysis of the Bow-tie antenna is presented in this section.

The characteristic impedance of a Bow-tie antenna is given by [59] as followings.

$$Z_{c,a} = 120 \ln \left(\cot \left(\frac{\theta_0}{4} \right) \right) \tag{3.1}$$

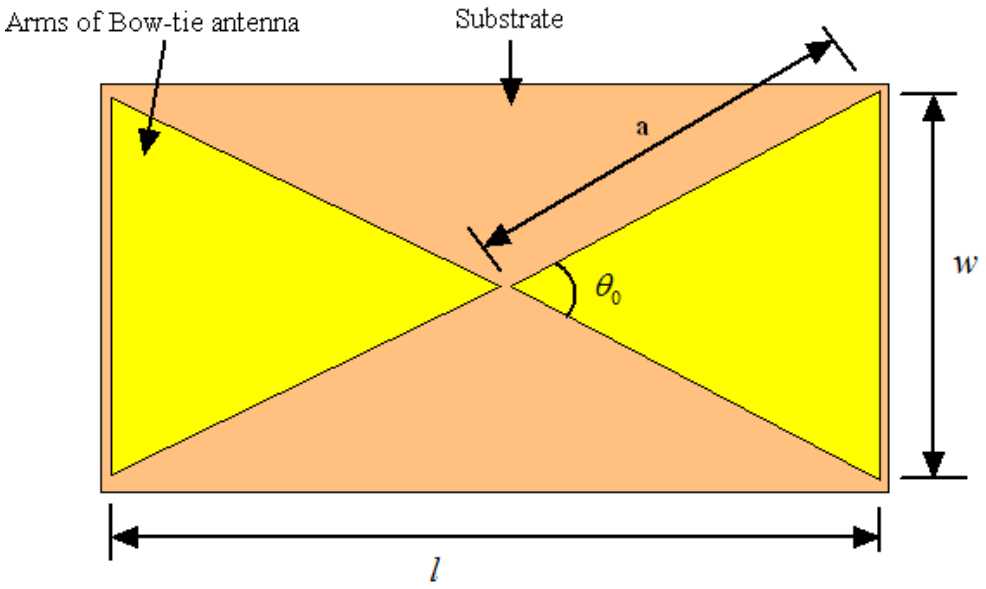

Figure 3.1: Basic geometry of a typical triangular Bow-tie antenna

where θ_0 is the opening angle (or flare angle) of each side. The length of the Bow-tie antenna can be determined by using the following equation [43].

$$l = \lambda_0 \times \left(\frac{1}{\sqrt{\varepsilon_{eff}}}\right) \tag{3.2}$$

where λ_0 is the wavelength corresponding to expected lowest operating frequency. The effective dielectric constant can be calculated by using the following expression [43].

$$\varepsilon_{eff} = \left(\frac{\varepsilon_r + 1}{2}\right) + (\varepsilon_r - 1)\left(1 + \left(10\frac{d}{w}\right)\right)^{-0.555} \tag{3.3}$$

where w= Bow-tie antenna width in mm, d=substrate thickness in mm, ε_r= dielectric constant of the substrate. Resonant frequency corresponding to the various modes of the Bow-tie antenna is given below [59].

$$f_r = c\frac{K_{mn}}{2\pi\sqrt{\varepsilon_r}} \tag{3.4}$$

where f_r= resonant frequency in Hz, K_{mn}= resonating modes, m and n are the number of modes, c = velocity of light in free space expressed in meter.

3.4 Design of Proposed Bow-tie Antenna

The design of the proposed antenna follows the design flow as in Figure 3.2. The Bow-tie antenna with extended arms as proposed in [48] is taken as the basic antenna in our design. Further, in the second stage, the basic design with extended arm is modified to minimize the end-fire reflections by rounding of the sharp corners as this leads to provide flatter input

impedance which can be easily matched in wide frequency band [51]. Lastly, in the third stage the antenna with extended arm and rounded corners is single-sided resistively loaded with the help of thin sheet of graphite to further enhance the bandwidth by lowering the lower cutoff frequency.

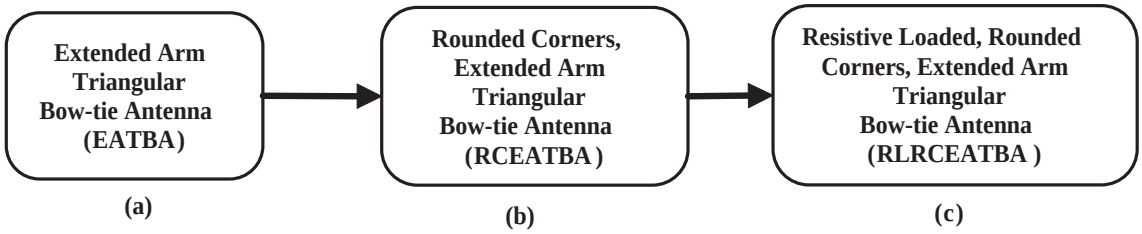

Figure 3.2: Design flow of the proposed antenna: (a) Basic Design with Extended Arms, (b) Improved Design with Rounded Corners, (c) Improved Design with Resistive Loading

The geometry of the proposed antenna is as shown in the Figure 3.3. The slot type structure is chosen as it provides an easy and better control over the radiation pattern of the antenna. The basic triangular Bow-tie antenna is modified with extended arms to achieve a wider bandwidth of operation and also incorporates triangular stubs with rounded corners so as to attain a better impedance matching with minimal end-fire reflections.

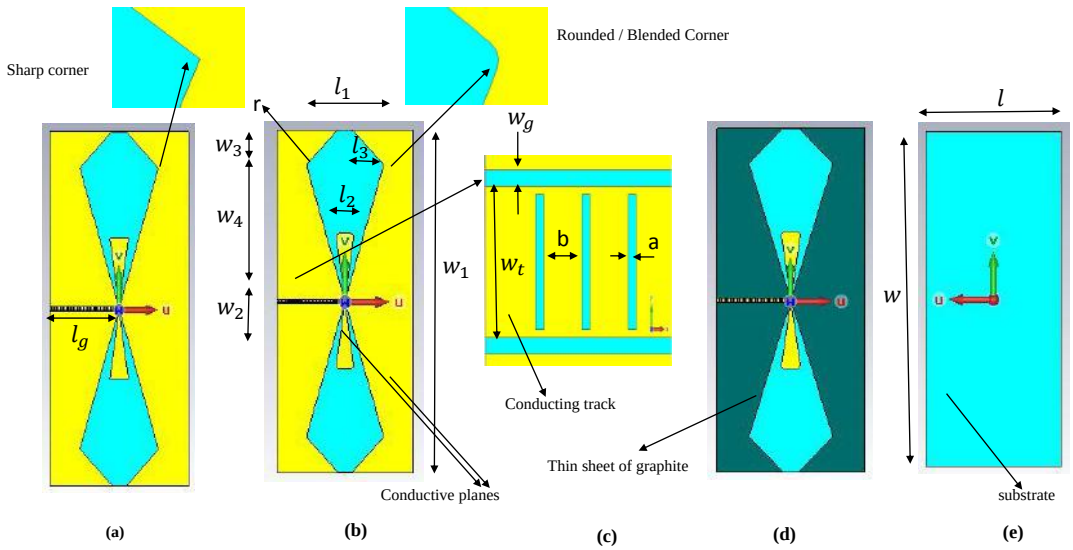

Figure 3.3: Geometries of proposed antennas: (a) Top view of the Basic Bow-tie antenna with Extended Arms, (b) Top view of the Improved Bow-tie antenna with Rounded Corners, (c) Top view of the CPW feedline, (d) Top view of the Improved Bow-tie antenna with Resistive Loading, (e) Bottom view of the all antennas

3.4.1 Design of Proposed CPW Feed line

The coplanar waveguide (CPW) feed line is chosen to be used for feeding the antenna for various advantages [60] i.e. ease of fabrication, easy control over characteristics impedance of the line, easy connection facility to the small miniature version A (SMA) connector, comparatively more bandwidth of operation. A cross sectional view of a typical ungrounded CPW line is shown in Figure 3.4.

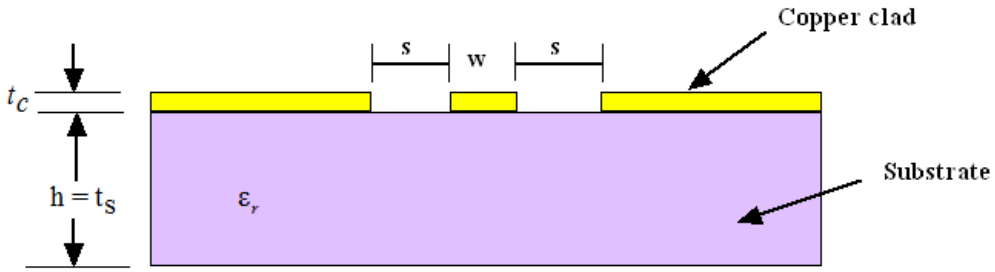

Figure 3.4: Cross sectional view of ungrounded CPW line

The characteristic impedance, Z_0, of the ungrounded CPW line is calculated by using different design equations specified in [60] as follows.

$$Z_{c,cpw} = \left(\frac{30 \times \pi}{\sqrt{\varepsilon_{eff}}}\right)\left(\frac{K\left(k'\right)}{K\left(k\right)}\right) \tag{3.5}$$

where effective dielectric constant of the substrate is given in 3.6.

$$\varepsilon_{eff} = 1 + \left\{\frac{(\varepsilon_r - 1)}{2}\right\}\left\{\left(\frac{K\left(k'\right)}{K\left(k\right)}\right)\left(\frac{K\left(k_1\right)}{K\left(k'_1\right)}\right)\right\} \tag{3.6}$$

$$k = \frac{w}{w + 2s} \tag{3.7}$$

$$k_1 = \frac{\sinh\left(\frac{\pi w}{4H}\right)}{\sinh\left(\frac{(w+2S)\pi}{4H}\right)} \tag{3.8}$$

$$k' = \sqrt{(1 - k^2)} \tag{3.9}$$

Here, K denotes complete elliptic integral of the first kind, w is the central strip width and S is the gap width of the CPW line.

The ratio of complete elliptic functions in Equation 3.5 can be approximated as either Equation 3.10 or Equation 3.11.

$$\frac{K\left(k\right)}{K\left(k'\right)} \approx \frac{1}{2\pi}\ln\left[2\frac{\left\{\sqrt{1+k} + (4k)^{\frac{1}{4}}\right\}}{\left\{\sqrt{1+k} - (4k)^{\frac{1}{4}}\right\}}\right] \quad for\ 1 \leq \frac{K}{K'} \leq \infty\ and\ \frac{1}{\sqrt{2}} \leq k \leq 1 \tag{3.10}$$

$$\frac{K(k)}{K(k')} \approx \frac{2\pi}{\ln\left[2\frac{\left\{\sqrt{1+k}+(4k)^{\frac{1}{4}}\right\}}{\left\{\sqrt{1+k}-(4k)^{\frac{1}{4}}\right\}}\right]} \quad for \;\; 0 \leq \frac{K}{K'} \leq 1 \;\; and \;\; 0 \leq k \leq \frac{1}{\sqrt{2}} \tag{3.11}$$

By using the design Equations the above equations, the values of the design parameters of the CPW line of characteristic impedance of 50 Ω are calculated so that the proposed antenna can be fed through a 50 Ω SMA connector. The CPW feed line has line width a=2.8 mm, slot width b=0.6 mm and is connected to the triangular stubs with rounded corners which helps in attaining better impedance matching as in Figure 3.3.

3.4.2 Design of Basic Design with Extended Arms

The antenna is designed on a single-sided copper clad FR4 substrate due to its easy availability and low cost. The thickness of substrate is t_s=1.6 mm and its relative dielectric permittivity ε_r =4.4 which are chosen so as to reduce the antenna size and to get wider bandwidth. The thickness of copper clad is t_c =0.035mm. The geometry of the basic design is as shown in Figure 3.3. The dimensions of the antenna are as follows. The width of the antenna is l=225mm, length of the antenna is w=505 mm. Other important parameters are l_1=127.4 mm,l_2=30 mm,l_3 =63.7 mm, w_1=503 mm,w_2=100 mm, w_3 =51.5 mm,w_4 =200 mm. The basic dimensions of the antenna are initially calculated for a resonant frequency of 1.5 GHz by using the design equations as given in Section 3.3. Then these parameters are further fine-tuned using parametric analysis and inbuilt optimizer present in CST Microwave studio v14.

3.4.3 Design of Improved Design with Rounded Corners

The sharp corners of the Bow-tie antenna causes end-fire reflections which results in the degradation of the radiation efficiency. Hence, the sharp corners of the arms are rounded or blended at an angle r=5^0 so as to minimize the end fire reflections. The blending angle is also chosen as based on parametric analysis and inbuilt optimizer of the CST Microwave Studio v.14. The geometry of the antenna with rounded corners are as shown in Figure 3.3.

3.4.4 Design of Improved Design with Resistive Loading

Late-time ringing phenomena which are potentially responsible for the masking of the buried targets in a GPR survey can be prevented by making the antenna resistively loaded [43]. In this paper, a resistive loading technique for enhancing the bandwidth of the proposed antenna by lowering the lower cutoff frequency is proposed as in Figure 3.3. It is achieved by covering the whole conducting portion of the copper clad by a thin sheet of graphite

having conductivity very less as compared to that of copper. In this process the overall surface resistance of the antenna reduces significantly. The thickness of the graphite layer is chosen as 1 mm which is obtained by the parametric analysis by the CST software. The antenna is resistively loaded only on printed side so that the radiation from the other side i.e. substrate side will be less affected. The radiation efficiency is slightly degraded due to resistive loading. The proposed antenna is placed in such a way that its conducting patch portion faces upward while the substrate side faces towards the ground so as to transmit more radiation to the ground. The compactness of the antenna is achieved with the help of single thin sheet of graphite instead of using more than one layer of volumetric absorbing materials .

The photos of the fabricated antenna are shown in Figure 3.5.

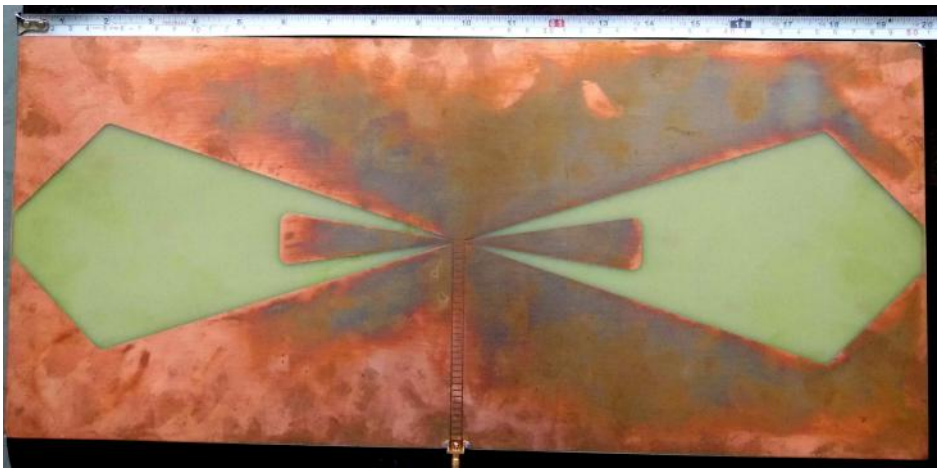

(a) without loading

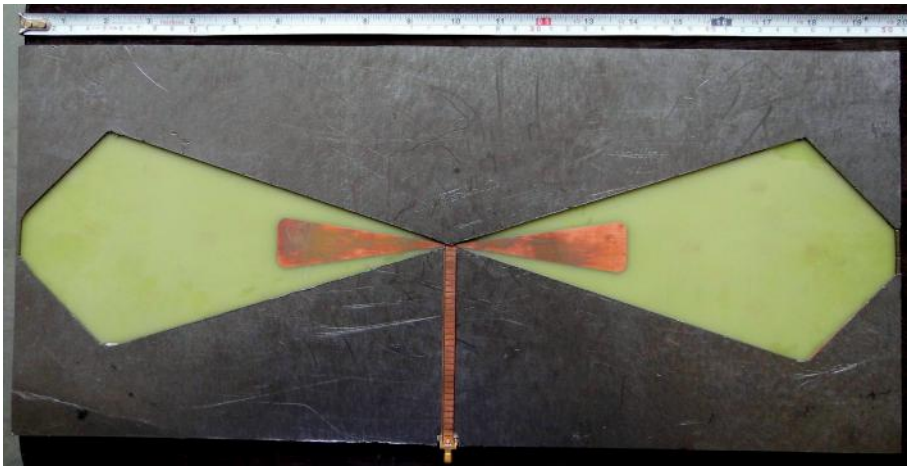

(b) with resistive loading

Figure 3.5: Photos of fabricated antenna

3.5 Results and Discussion

Firstly, the proposed antenna is designed and simulated in Computer simulation technology (CST) Microwave studio v.14 with the help of a PC having octa core i5 processor with 8 GB RAM. Then, it is designed and simulated in HFSS (High frequency structure simulator) v14 using High Performance Computing (HPC) cluster with 32 computing nodes (Intel Xeon 2.0 GHz, two CPU 16 cores, 64GB) facility available in the institute. A comprehensive analysis of simulation and measurement results are discussed in this section.

3.5.1 Simulation Results

The initial design parameters of the proposed antenna are fine-tuned with the help of parametric analysis by CST Microwave studio v14 and are also optimized by the inbuilt time domain optimizer of CST Microwave studio v14 which uses a trust region framework algorithm. A similar approach is followed for the design and simulation of the proposed antenna in HFSS v14. Design and simulation of the proposed antenna are carried out rigorously so that the fabricated antenna will provide antenna performance close to the simulated results. The proposed antenna provides an impedance bandwidth of 169 % (0.4 GHz - 4.8 GHz) measured with respect to S_{11} = -8 dB level and impedance bandwidth of 118% (1.2 GHz - 4.7 GHz) measured with respect to S_{11} = -10 dB level with the help of resistive loading and rounded corners with a best case gain of 7 dB and worst case gain of 4 dB. The results obtained for various antenna performance parameters from CST Microwave studio v14 and HFSS v14 are presented as follows.

(a) **S_{11} Performance**: The S_{11} performance obtained from CST and HFSS given in Figure 3.6 shows a high degree of similarity throughout the said band. However, HFSS provides 8 % more frequency band of operation with respect to S_{11} = -10 dB level and 38 % more frequency band of operation with respect to S_{11} = -8 dB level due to resistive loading and rounded corners. Specifically, due to resistive loading the lower cutoff frequency is shifted from 1.3 GHz to 0.4 GHz.

(b) **Gain**: Result obtained from CST and HFSS shows that the maximum of 7 dB at the frequency of 2.5 GHz while the minimum gain of the antenna throughout the said band is more than 2.8 dB as shown in Figure 3.7. However, the gain of the improved design with resistive loading is slightly degraded as compared to that of improved design with rounded corners due to resistive loading effect while it provides an extension of bandwidth in the low frequency range.

(c) **Directivity**: The directivity throughout the said band is more than 4.2 dBi obtained as shown in Figure 3.8. Directivity of the improved design with resistive loading is

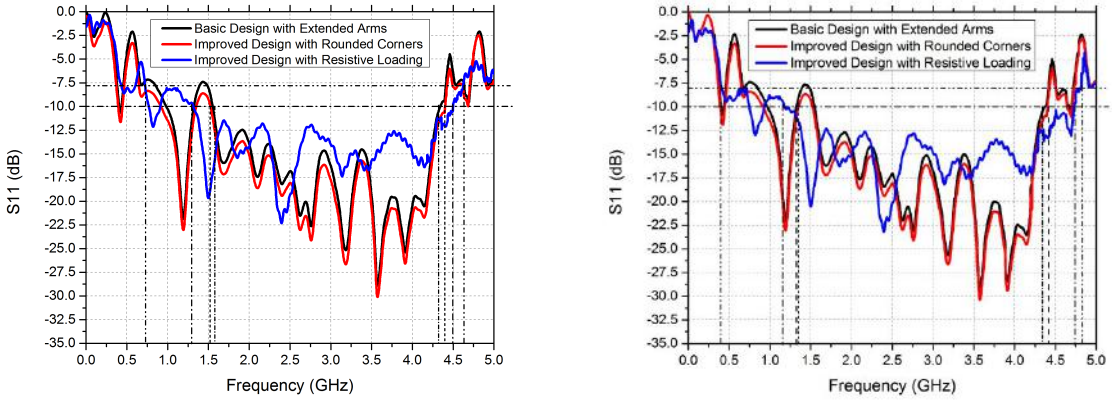

(a) Obtained from CST (b) Obtained from HFSS

Figure 3.6: S_{11} Vs Frequency plots

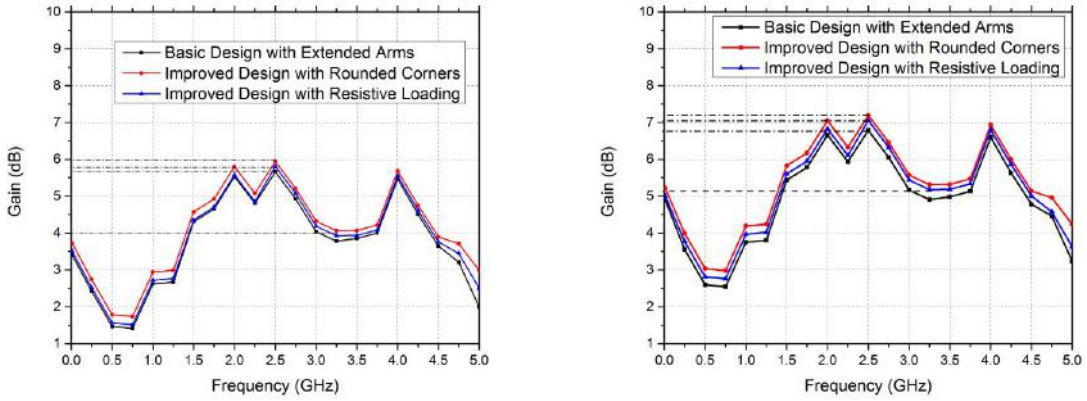

(a) Obtained from CST (b) Obtained from HFSS

Figure 3.7: Gain Vs frequency plots

slightly less than that of the improved design with the rounded corners due to loss in resistive loading.

(d) **Efficiency**: Radiation efficiency is more than 71 % with respect to S_{11} = -10 dB level and more than 60 % with respect to S_{11} = -8 dB level as shown in Figure 3.9. Total efficiency is more than 60 % with respect to S_{11} = -10 dB level and more than 55 % with respect to S_{11} = -8 dB level as shown in Figure 3.9. The total efficiency is slightly less than the radiation efficiency as total efficiency calculation includes different losses such as parasitic emission, thermal losses, etc. Due to the introduction of rounded corners, the minimum radiation efficiency of the improved design with rounded corner is 90 % which denotes the reduced end-fire reflections.

(e) **Farfield radiation patterns**: The farfield radiation patterns for E-plane and H-plane patters of the proposed antenna are summarized in Table 3.1. It shows that the E-Plane

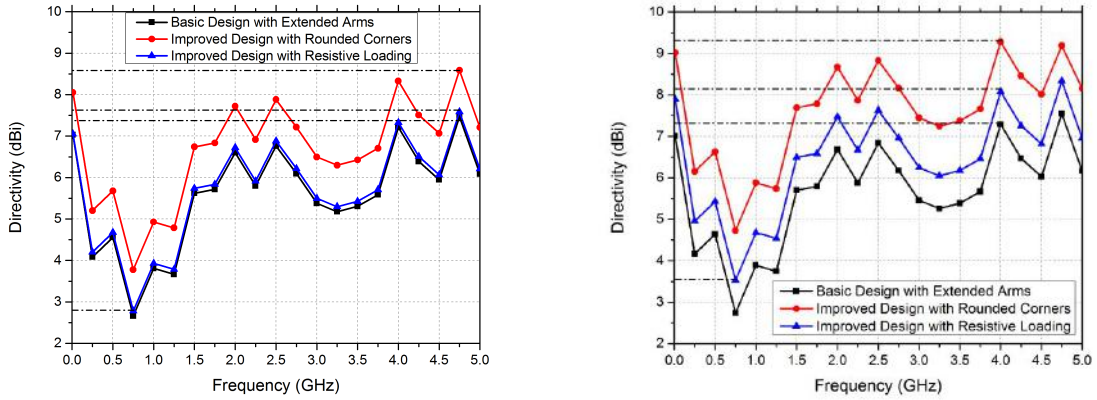

(a) Obtained from CST (b) Obtained from HFSS

Figure 3.8: Directivity Vs frequency plots

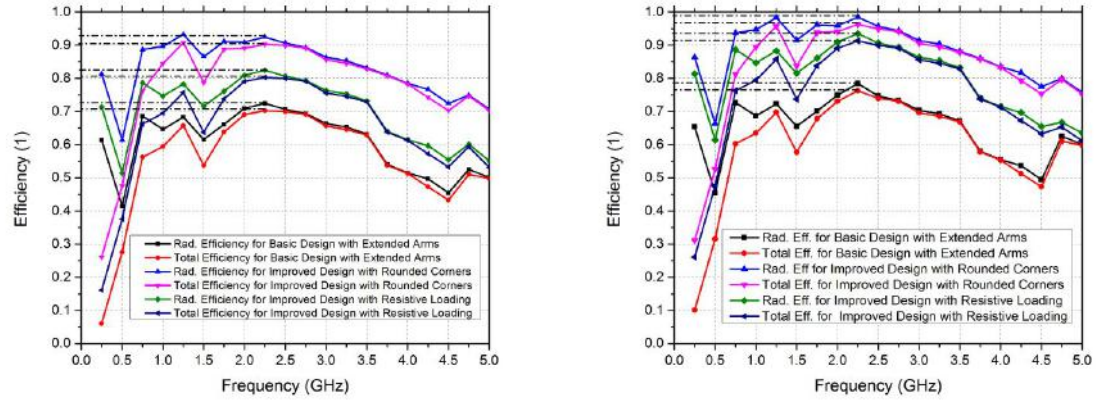

(a) Obtained from CST (b) Obtained from HFSS

Figure 3.9: Efficiency Vs frequency plots

has maximum gain of 6.08 dB and H-Plane has maximum gain of 2.46 dB.It also shows that proposed antenna has narrow beam width compared to [6] which is also a required characteristic of the UWB antenna. The farfield radiation patterns for E-plane and H-plane are summarized in the Table 3.1. The polar plots of farfield radiation patterns for the worst case at frequency of 0.5 GHz is as shown in Figure 3.10 shows that the proposed antenna has E-plane pattern which is bidirectional and H-plane pattern which is omni-directional which are similar to the dipole with improved gain, efficiency and directivity.

3.5.2 Measurement Results

The measured results for the fabricated antenna are shown in Figure 3.11. The measured reflection coefficients of the fabricated antenna without resistive loading and with resistive

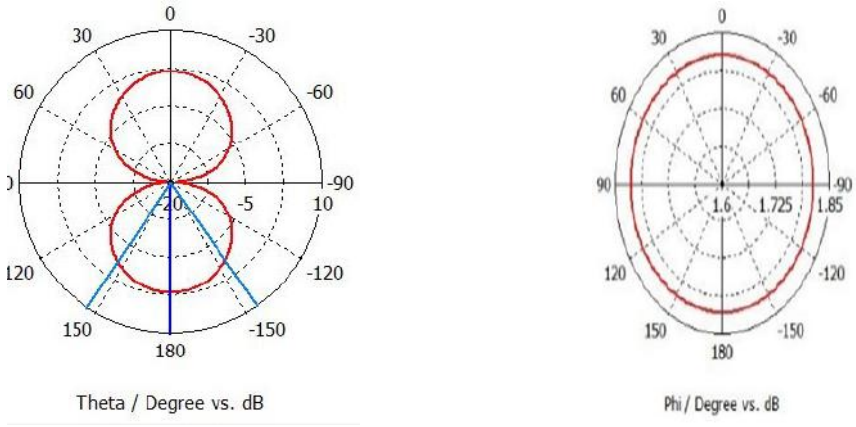

(a) E-plane pattern (b) H-plane pattern

Figure 3.10: Far field radiation patterns at f= 0.5 GHz

Table 3.1: Farfield results of the proposed Antenna

Freq. (GHz)	E-plane			H-plane		
	Main lobe Magnitude,(dB)	Main lobe Direction,(deg.)	Angular,(3 dB) Beam Width,(deg.)	Main lobe Magnitude,(dB)	Main lobe Direction,(deg.)	Angular (3 dB), Width,(deg.)
0.5	1.82	180	68.9	1.81	144	40.5
1	2.99	-38	39.9	1.39	-57	30.8
1.5	4.57	-37	29.6	-0.735	-35	18.5
2	5.72	-50	29.8	0.838	-85	45.4
2.5	6.04	-57	23.8	2.35	80	30.8
3	3.6	-87	97.1	3.64	-94	23.2
3.5	3.9	-70	87.3	4.02	91	20.6
4	5.68	109	22.4	3.93	-91	21.2
4.5	3.22	-88	38.6	3.21	-95	29.6

loading are measured with the help of vector network analyzer, i.e.VNA (E5071C of Agilent). The measured results show a high degree of similarity with simulated results. Due to the operational frequency range limitation of the VNA, the measurement is carried out for a range of 5 MHz to 4.5 GHz. The little amount of mismatch may be due to use of locally available FR4 substrate and adhesive used to attach the graphite sheet on the antenna.

3.5.3 Discussion

The results obtained from CST (Computer Simulation Technology) Microwave studio v14 and HFSS (High Frequency Structure Simulator) v.14 exhibit a high degree of similarity as shown in Table 3.2. Again, the measured S_{11} also shows a good degree of matching with the simulated results. This provides us a good amount of confidence that the other antenna performance parameters of the fabricated antenna will provide antenna performances close to the simulated results.

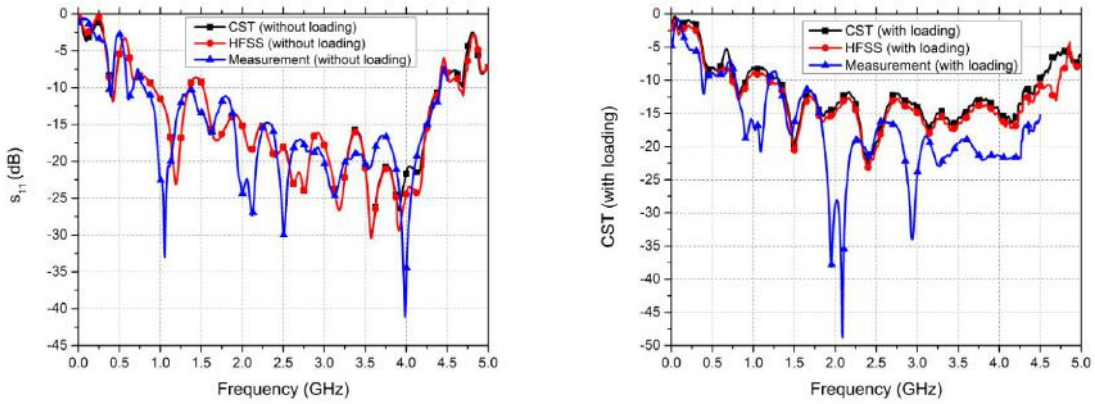

(a) For the antenna without loading

(b) For the antenna with loading

Figure 3.11: Measurement results of the designed antenna

3.6 Thermal and Mechanical Coupled Simulation of the Proposed Antenna

Usually, maximum of the GPR applications are surveys involved in field or outside of the room condition such as road inspection, soil moisture estimation, etc. Hence, there is a high probability that the antennas have to expose to the various extreme conditions of the temperature variations and this may results in the physical or mechanical deformation of the antenna. There is also another possibilities of increase in temperature inside the antenna body due to continuous flow of RF signals across it. Therefore to study the impact of the temperature variations inside the antenna body and its surrounding and the mutual exchange of heat energy between the antenna with its surrounding is simulated in Thermal and Mechanical solvers of CST studio in multi-physics environment . The simulation of the antenna in the normal conditions are done under the ideal condition assumptions, i.e. (a) Constant temperature across the antenna body and its surrounding part of antenna, and (b) there is no effect of mechanical properties of the antenna on the antenna body. The variations of the thermal and mechanical effects to the whole antenna body can be controlled by the scaling factor in the simulation level and the value of this scaling factor can be selected depending upon the applications of the GPR antenna. The impact of the thermal and temperature variations on the antenna is indicated in the reflection coefficient plot of the antenna as shown in Figure 3.12. From this, it can be concluded that the proposed antenna is not prone to thermal and mechanical effects.

Table 3.2: Comparative analysis of the obtained results from CST and HFSS

Antenna Parameters			Resulted from CST	Resulted from HFSS
Results with respect to S_{11} = -10dB level	Cutoff frequencies (GHz)	F_L	1.3	1.2
		F_H	4.5	4.75
	BW %		110.34	119.32
	Gain (dB)	Max.	5.8	7
		Min.	4	5.2
	Directivity (dBi)	Max.	7.8	8.2
		Min.	4.2	3.8
	Radiation Efficiency (%)	Max.	81.5	94
		Min.	71	74
	Total Efficiency (%)	Max.	80.5	92
		Min.	64	74
Results with respect to S_{11}= -8dB level	Cutoff frequencies (GHz)	F_L	0.75	0.4
		F_H	4.65	4.8
	BW %		121.87	169.23
	Gain (dB)	Max.	5.8	7
		Min.	1.6	2.8
	Directivity (dBi)	Max.	7.8	8.2
		Min.	2.8	2.75
	Radiation Efficiency (%)	Max.	81.5	94
		Min.	60	60
	Total Efficiency (%)	Max.	80.5	92
		Min.	60	55

3.7 Performance Analysis of the Proposed Antenna in GPR Scenario

Generally, antennas are designed to couple the signal into the air medium where as the GPR antennas are designed to couple the whole signal in to the host media, i.e. soil, concrete, etc. Hence, the whole approach for the design of the GPR antennas significantly differs from that of the antenna applicable for the wireless communication, air borne radar systems, etc. Further, the GPR antenna design has to take care of various constraints imposed by the host media, applications, desired resolution and range, etc. To study the effectiveness of our antenna in GPR environment, the antenna is simulated in the GPR scenario created tn the CST Microwave studio v.15 as shown in Figure 3.13. For design simplicity the ground is considered to 3 layered media.Layer 1 is dry and sandy soil (ϵ_r =2.53, μ_r =1, σ=0.0036), layer 2 is wet and sandy soil (ϵ_r =13, μ_r =1, σ=0.29), and layer 3 is dry and sandy soil (ϵ_r =13.80, μ_r =1, σ=0.18).The top two layers have thickness of 10 mm and 15 mm while the bottom layer is taken as infinite in depth.

The S_{11} performance of the antenna in GPR scenario is compared with that of the antenna in the free space conditions as shown in Figure 3.14. It is indicative that the S_{11} in GPR

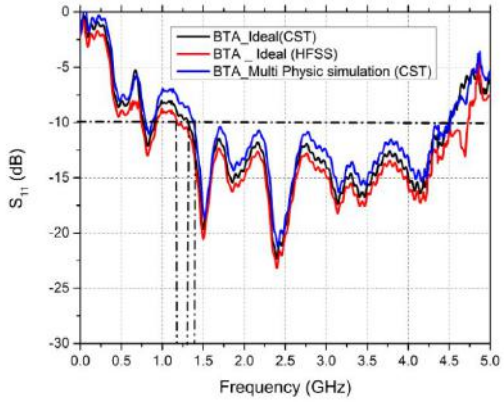

Figure 3.12: Thermal and mechanical solver analysis of the proposed R-loaded Bow-tie antenna

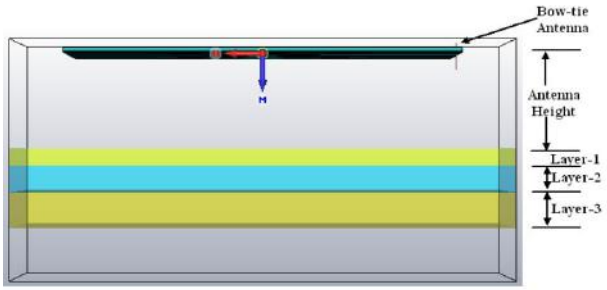

Figure 3.13: R-loaded Bow-tie antenna in GPR scenario

scenario is differed significantly from that of the antenna in air medium. More specifically, the antenna performance is deviated significantly in the low frequency range due to the low pass nature of the host media. However, low frequency components are very much useful for the large penetration depth. Hence, it can be concluded that the design of the GPR antenna should be application specific, i.e. it has to be designed for a specific medium having particular dielectric constant.

3.8 Comparison of Performances of Proposed Antenna with Existing Antennas

Since the fabricated antenna couldn't be tested in anechoic chamber for free space measurement, the simulated and partially measured results are compared with the simulation results of existing antennas in literature as presented in Table 3.3. The antenna performance of the proposed design is found to be promising compared to the antenna performances

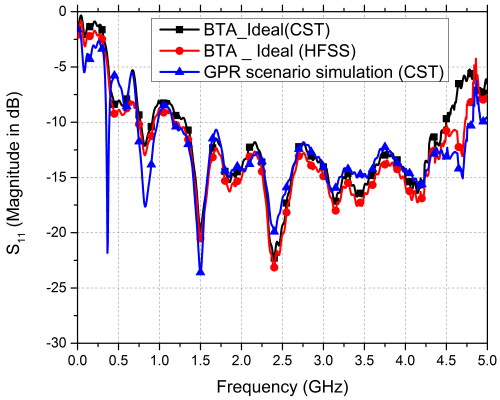

Figure 3.14: S_{11} performance of the R-loaded Bow-tie antenna in GPR scenario

reported in the various literatures.

Table 3.3: Comparative analysis of performance of proposed antenna with pre-existed antennas

Design Proposed by	F_L (GHz)	F_H (GHz)	BW (%)	Max Gain (dB)	Min Gain (dB)	Overall Size (cm^3)
[12]	0.3	3	163.63	6, 12 (with lens)	-10	$50 \times 20 \times 4$
[24]	0.055	1.5	185.8	...	...	$40 \times 40 \times 10$
[48]	0.4	1.5	115.8	6	2.5	$50 \times 22 \times 15$
[47]	0.46	4	158.7	4.2	2	$36 \times 23 \times 7$
[46]	0.25	0.75	100	8	2.6	$18 \times 30 \times 8$
Proposed Design	0.4	4.5	167.34	7	2.8	$51 \times 22 \times 0.5$

3.9 Summary

An improved design of Bow-tie antenna, i.e. resistively loaded, compact, CPW-fed slot Bow-tie antenna which can operate through a wide bandwidth of 4.1 GHz is proposed. The sharp corners of the slot antenna are rounded so as to minimize the end-fire reflections. The proposed antenna employs a resistive loading technique through a thin sheet of graphite to attain the ultra-wide bandwidth. This antenna can provide better resolution due to its UWB nature and lager depth of penetration due to its low value of lower cutoff frequency. The overall efficiency of the GPR system may be enhanced significantly by using the proposed antenna as its worst case radiation efficiency is 71%. The proposed antenna with enhanced bandwidth, reduced end-fire reflections and compactness has advantageous for GPR application requirements. The measurement results for the S_{11} performance or return loss shows a good agreement with the simulated one. The slight degradation of the measured results might be due to the lossy nature of the cable. The future work should focus on the measurement of the antenna in the anechoic chamber and testing of proposed antenna in the practical GPR scenario.

However, major limitation of this work is the degradation of gain due to resistive loading. This can be improved significantly by using a combination of resistive loading and capacitive loading, i.e. RC-loading scheme which will be discussed in the Chapter 4.

Chapter 4

Design and Analysis of RC-loaded Bow-tie Antenna with Meta-material Lens

4.1 Introduction

The resistive loading alone is able to enhance the bandwidth of the antenna by lowering the lower cutoff frequency of the antenna at the cost of radiation efficiency. However, the GPR antenna should possess high radiation efficiency to receive the reflected signal effectively. The capacitive loading alone is able to increase the bandwidth of the antenna without decreasing the radiation efficiency significantly with considerable amount of ringing. Hence, there is a requirement of improved RC-loading (combination of both resistive and capacitive loadings) which can provide UWB and ringing free performance without decreasing the radiation efficiency significantly. Generally, the ordinary Bow-tie antennas are not able to provide high gain and directivity which are very much essential for the GPR applications. Hence, in this work, an improved RC- loaded compact Bow-tie antenna with metamaterial lens having UWB performance is intended to be designed for the GPR applications.

The rest of the chapter is organized in the following manner. The related works to the RC-loaded Bow-tie antennas are briefly presented in the Section 4.2. A theoretical analysis of the half elliptical bow-tie antenna id discussed in Section 4.3. In Section 4.4, the design of the improved RC- loaded half-elliptical Bow-tie antenna (HEBTA) with metamaterial (MM) lens is discussed in detail. The simulation results obtained for various antenna performances are presented in section 4.5. The performance analysis of the antenna in temperature varying environment and GPR scenario are investigated with the help of CST Microwave studio v. 15 in the simulation level as discussed in the sections 4.6 and 4.7. A comparative analysis of the proposed antenna is presented in the section 4.8 followed by the conclusion of the chapter in section 4.9.

4.2 Related Work

Antennas are used in a close proximity of the ground so to couple more amount of energy to the ground. The GPR should able to transmit pulses having minimal late-time ringing so that the masking of the targets can be prevented. The abrupt change in impedance level of the either sides of the Bow-tie antenna causes late-time ringing, i.e., multiple reflection between the feed point and the open end of the Bow-tie antenna. This indicates the narrow band performance of the antenna [40]. Resistive loading techniques have been successfully applied to increase the bandwidth and hence minimizing late-time ringing as reported in [30, 33]. But, the major limitation of the resistive loading is reduction of the radiation efficiency significantly [40]. Many researchers also tried to increase the bandwidth and minimize the ringing with help the capacitive loading scheme without decreasing the radiation efficiency [35], however, this technique exhibits a relatively high level of ringing [40]. Hence, the GPR antenna should possess high efficiency so as to decrease power consumption and to receive the reflected signals with high amplitude. This is due to the fact that the antenna with high efficiency can transmit the pulse having an amplitude very much close to that of the excitation pulse. This will ultimately help to detect the target buried in lossy media as the transmit pulse can manage an extra amount of loss of energy and the probability of getting reflected signal having an amplitude greater than the noise floor will be more. Hence, there is a requirement of the Bow-tie antenna with high efficiency and minimal ringing. This can be achieved with the help of the composite loading known as RC-loading which is a combination of both resistive loading and capacitive loading as reported in [6, 12, 40]. A novel and efficient one sided RC-loading scheme comprises of a constant resistive loading realized with the help of volumetric microwave absorbing materials and linear capacitive loading realized by creating narrow concentric slots having different widths is reported in [40]. However, its lower cutoff frequency is 0.5GHz, which comparatively high for GPR applications and the frequency domain analysis of the reported antenna is not presented. Recently, a compact UWB Bow-tie antenna with meta-material lens is reported in [6, 12]. The high gain and directivity of the antenna which operates in UHF band are achieved with the help of planar meta-material lens. However, the gain of the reported antenna decreases significantly after 1.5 GHz.

In this work, an improved and partially covered RC-loading technique scheme is utilized with the modified form of planar meta-material lens as reported in [6] to achieve UWB performance from 0.29 GHz to 4 GHz with a minimum gain of 1.5 dB throughout the said band.

4.3 Theoretical Analysis of Half-elliptical Bow-tie antenna

Ideally, the bow-tie antenna is a frequency independent antenna as it is infinite in length and specified only by angles. The characteristic impedance of the Bow-tie antenna primarily depends upon the flaring angle. Many bow-tie antennas which have triangular structure are designed for the input impedance of 100 Ω due to its linear flaring angle [6]. It is always a difficult task to design a wide band feed line with an impedance transformation from 50 Ω to 100 Ω having a minimum reflection coefficient. The triangular Bow-tie antenna is also not a very much better structure to obtain UWB performance due to its sharp corners responsible for end-fire reflections. Hence, Bow-tie antennas have been studied by many researchers to improve the antenna performance. Conformal mapping, i.e. angle preserving transformation is a widely used analytical method used to study the Bow-tie antenna systematically [6] Recently, it is reported that frequency independent antennas such as Bow-tie antenna can be transformed into a pair of coplanar strip lines with the help of conformal mapping [6, 61]. The derivation of the expression for the characteristic impedance of the infinite length fin antenna is reported in [62]. Due to numerous constraints, the broadband Bow-tie antenna is finite, having stable radiation characteristics over a bandwidth [6]. A brief theoretical analysis of the half-elliptical Bow-tie antenna (HEBTA) is presented in [6]. A Bow-tie antenna can be represented in the polar coordinates as given in Equation 4.1.

$$z = re^{j\theta} \tag{4.1}$$

where θ is flaring angle and r is the radius of the Bow-tie antenna. This analytic function is conformally mapped into w-plane by the following function.

$$\omega = \ln r + j\theta \tag{4.2}$$

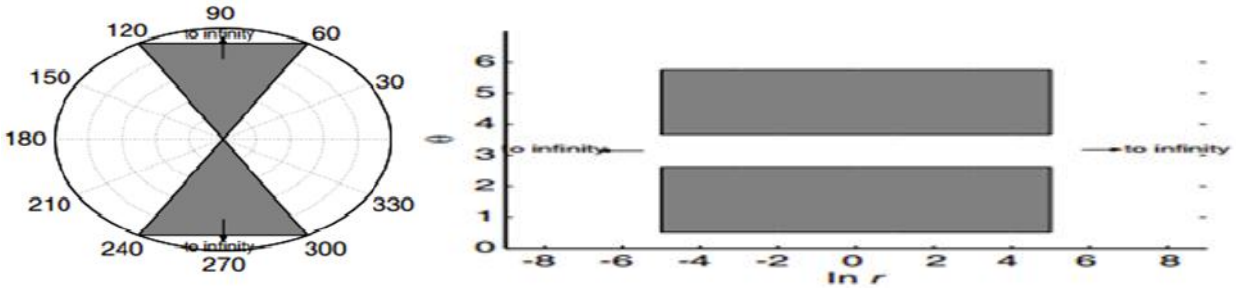

(a) Infinite Bow-tie antenna (b) Conformal transformed version of (a)

Figure 4.1: Conformal transformation of infinite Bow-tie antenna [6]

The conformal transformation for the infinite Bow-tie antenna and elliptical Bow-tie antenna are shown in Figure 4.1 and Figure 4.2 respectively as reported in [6].From this conformal analysis, it is found that the characteristic impedance of the infinite length Bow-tie

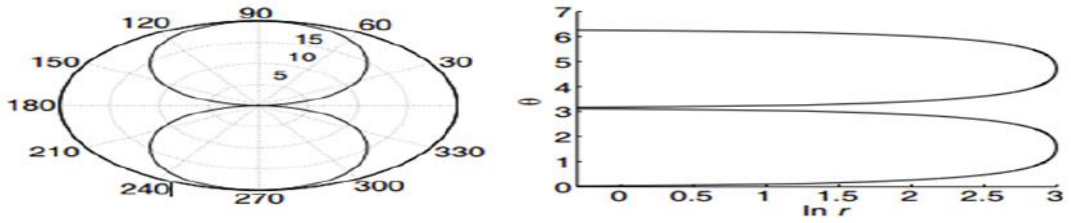

(a) Elliptical Bow-tie antenna (b) Conformal transformed version of (a)

Figure 4.2: Conformal transformation of elliptical Bow-tie antenna [6]

antenna remains constant, whereas that of the elliptical antenna gradually decreases due to decrease in ratio of gap 'a' to total feed line width 'b'. This results that the elliptical Bow-tie will initially have less characteristic impedance as the impedance of the Bow-tie antenna is inversely proportional to the flare angle [62]. Hence, the input impedance of the half-elliptical Bow-tie antenna is smaller than that of the triangular Bow-tie antenna due to the non-linear flaring nature of the elliptical structure. This facilitates the ease of impedance matching. The elliptical shape of the antenna also provides a smooth path for the current flow across the antenna. This helps in attaining UWB performance of the antenna [11]. Hence, half elliptical structure is chosen as the shape of the Bow-tie arm as reported in [6, 12, 46].

4.4 Design of the RC-loaded HEBTA with Meta-material Lens

The complete design process of the improved RC-loaded HEBTA can be divided into three stages as shown in Figure 4.3. In stage-1, design of the basic half-elliptical bow-tie antenna (HEBTA) with the required feed network is carried out. In this stage, the major task involves the design of UWB balun (balanced to unbalanced) transformer for feeding of the HEBTA. In stage-2, a composite improved RC-loading scheme realized by the combination of various loading schemes is carried out. The prime focus of this stage is to design and implement an improved RC-loading scheme which can provide the UWB performance by lowering the lower cut-off frequency without decreasing the radiation efficiency significantly. In stage-3, an improved metamaterial based unit cell is designed and a meta-material based planar lens is integrated with the RC-loaded HEBTA. The prime objective of this work is to increase the directivity and hence gain of the RC-loaded HEBTA by utilizing the focusing action of the metamaterial based planar lens.

The physical dimensions of the improve RC-loaded HEBTA with metamaterial lens are as given in the Table 4.1. The detailed explanation of the individual stages are as follows.

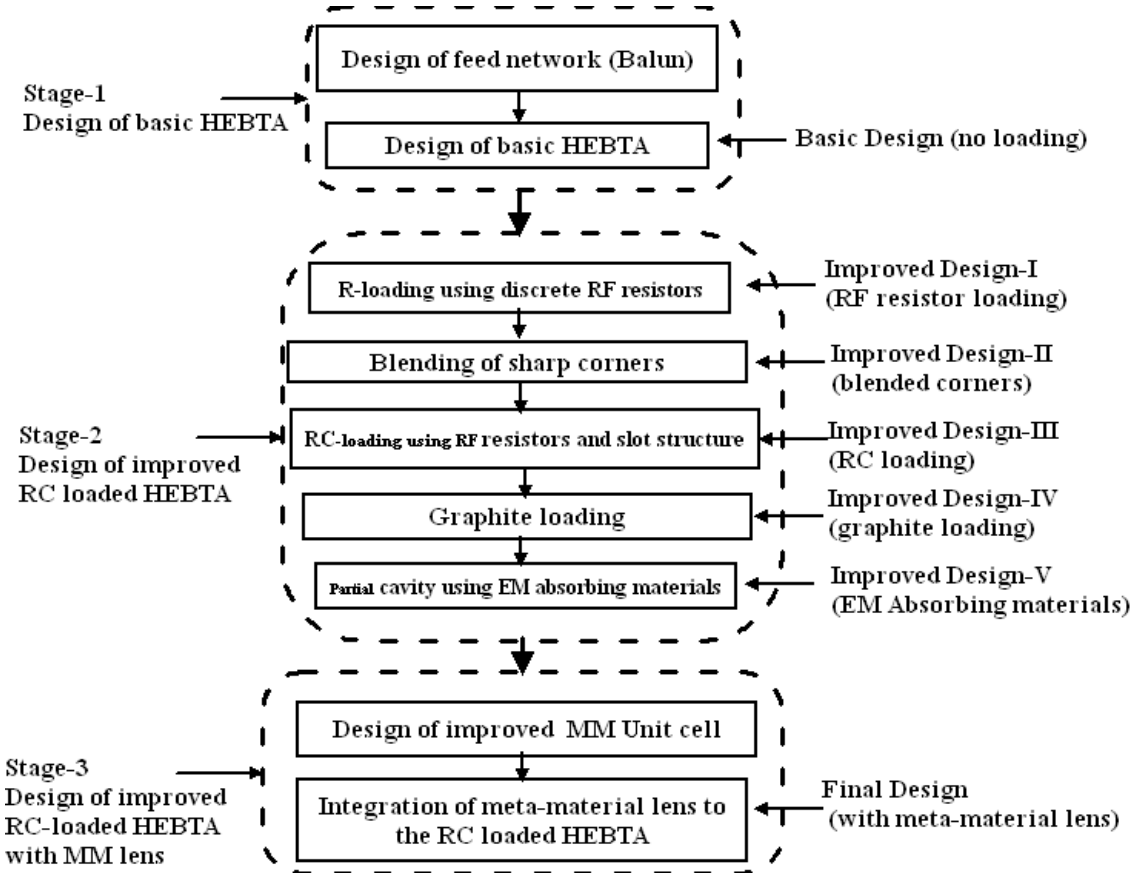

Figure 4.3: Design flow of the improved RC-loaded HEBTA with MM lens

4.4.1 Stage 1: Design of the basic HEBTA with its feed network

In this stage-1, basic HEBTA and a feed network for providing the balanced feeding to it are designed using CST Microwave studio v.15. The detailed descriptions of the each of steps is discussed as follows.

(i) Design and analysis of MPL to DSPSL Balun

The Bow-tie antenna is being similar to the dipole antenna is a balanced or symmetrical antenna. The direct connection of the Bow-tie antenna with the coaxial cable results in an unbalanced or asymmetrical driven system [63]. The input impedance of the bow-tie antenna

Table 4.1: Design Parameters of the RC loaded HEBTA with Metamaterial lens (in mm)

$t_s = 1.6$	$t_c = 0.035$	$t_g = 1$	$t_a = 15$	$a_h = 147$
$b_h = 112.5$	$g_1 = 1.6$	$g_2 = 2.5$	$g_3 = 0.75$	$h_m = 14.4$
$l_m = 300.6$	$w_m = 230$	$L_a = 300.6$	$W_a = 230$	$H_a = 66$
r = 10	$w_1 = 2.3$	$w_2 = 2.1$	$w_3 = 1.9$	$s_1 = 2.7$
$s_2 = 2.9$	$w_f = 20$	$l_f = 50$		

is primarily depends upon the flaring angle and it is optimized to 100 ohms in many reported designs due to the linear flaring nature of their arms [12]. The wideband performance of the antenna is primarily dependent on the feed network bandwidth [64]. Hence, there is a requirement of a balun (balance to unbalance) which is used to convert the unbalanced current flow of the coaxial cable to the balanced current flow of two symmetrical lines used for the exciting the Bow-tie antenna [65, 66]. Hence, to achieve the UWB performance of the proposed antenna, an improved wideband feed network, i.e. microstrip line (MPL) to double sided parallel strip line (DSPSL) is designed and used for the exciting the antenna as reported in [12, 67]. The sectional views of the typical MPL and DSPSL are shown in Figure 4.4. The DSPSL is chosen instead of coplanar strip line as it possess attractive features [67]: simple structure for wide band transitions, ease of realization of low characteristics transmission line, and good performance when balance current is required.

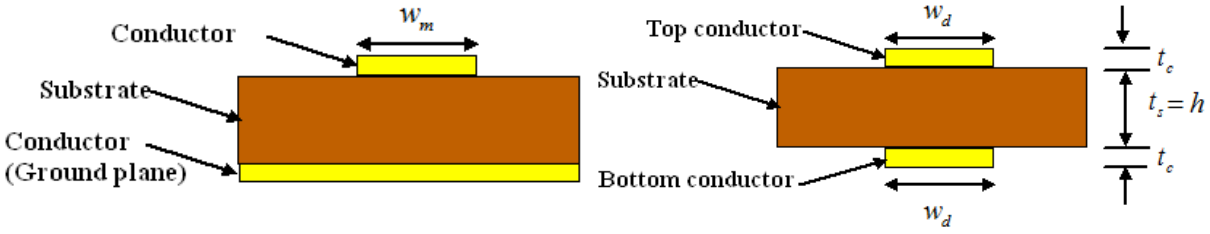

(a) Sectional view of MPL (b) Sectional view of DSPSL

Figure 4.4: Transmission lines used in the balun

The balun is designed on a copper cladded (thickness of copper=0.035 mm) FR4 substrate having dielectric constant 4.4 and thickness 1.6mm. The width of the 50 ohm microstrip line wm is calculated by using the design equations as mentioned in [65, 68]. The width of the DSPSL is calculated by using the basic concept, i.e. "for the same strip width, the characteristic impedance of the DSPSL with dielectric thickness 'h' is twice the characteristic impedance of the microstrip line with dielectric thickness h/2" as reported in [67]. Further, the strip width of the DSPSL is optimized by the inbuilt time domain optimizer of the CST Microwave studio v. 15 due to the use of a non-linear flaring of the Bow-tie antenna to achieve the UWB performance. The ground plane of the balun is tapered so as to attain the impedance transformation from the 50 ohm MPL to 100 ohm DSPSL with minimum

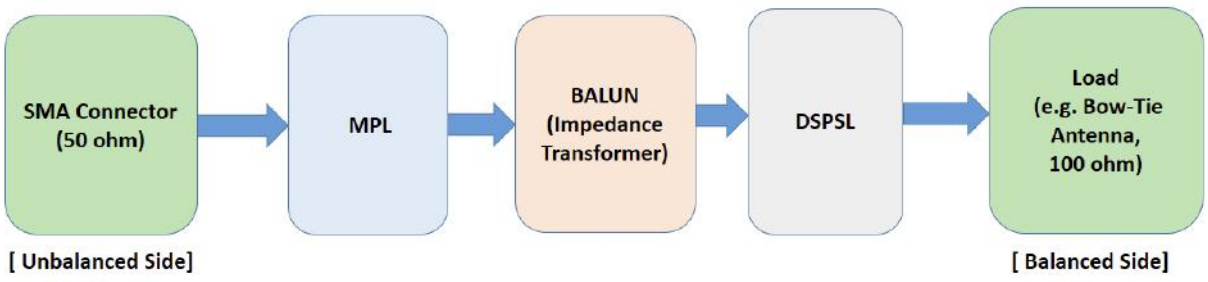

Figure 4.5: Basic principle of operation of the Balun

Table 4.2: Design parameter of the Balun in mm

w_m	3	w_f	20	l_t	3	l_d	10
w_d	2.4	l_f	50	l_m	10	r	90

reflection coefficient.Due to the non-linear flaring provided by the half-elliptical structure of the patch, the impedance of the Bow-tie antenna reduces to 74.8 Ω and corresponding width of the DSPSL is obtained by parametric and optimization analysis using CST Microwave studio. The radius of the curvature for the tapering profile is optimized with the help of inbuilt optimizer of the CST Microwave studio v.15. The physical dimensions of the balun are as shown in Table 4.2. below.

The designed balun and its S-parameter performances are as shown in Figure 4.6. The results clearly indicate that throughout the required frequency band of operation (0.25 GHz to 5 GHz), the S_{11} value lies below -10 dB and hence it can be used as the feeding network. It is placed perpendicular manner to the antenna so as to achieve better symmetry in the radiation pattern.

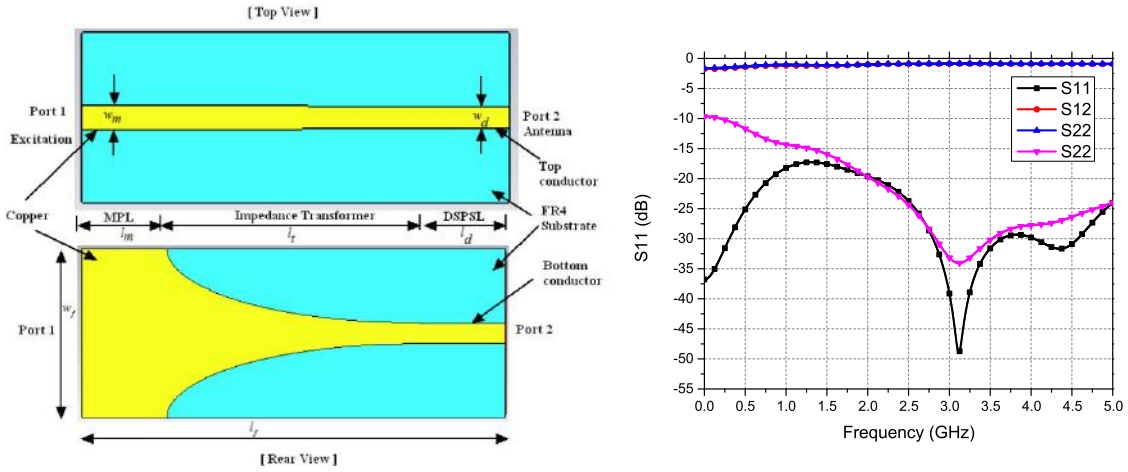

(a) Design of MPL to DSPSL Balun

(b) S-parameter performance plots

Figure 4.6: MPL to DSPSL Balun

The balun performance is also tested in the simulation level by simulating it in back-to-back configuration as this configuration facilitates the measurement of the return loss and insertion loss without the use of loads. The back-to-back configuration of the balun with its S-parameter performance plots are shown in Figure 4.7. The insertion loss and return loss of the balun are found to be below 10 dB and 2.5 dB respectively throughout the whole band which indicates the UWB nature of the balun.

(ii) Design of Basic HEBTA

All the initial parameters of the basic half-elliptical Bow-tie antenna are calculated corresponding to the expected low frequency 300 MHz by using the design equations for

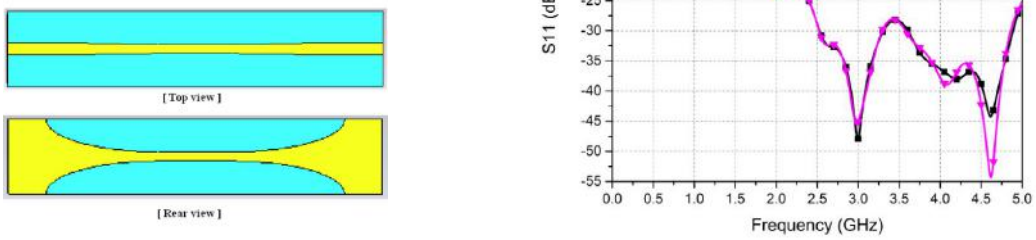

(a) Design of back-to-back configuration of the Balun (b) S-parameter performance plots

Figure 4.7: Back-to-back configuration of the MPL to DSPSL Balun

the Bow-tie antenna as given in Chapter 3. The antenna is designed on a single sided copper coated (copper thickness is 0.035 mm) FR4 substrate having dielectric constant 4.4 and thickness 1.6 mm using CST Microwave studio v.15. The design parameters are finalized by using parametric analysis and inbuilt optimizer of the CST Microwave v.15. The feedline is placed perpendicularly to the antenna so as to attain symmetric radiation pattern due to balanced matching of the impedances.The front view and perspective view of the basic HEBTA are shown in Figure 4.8.

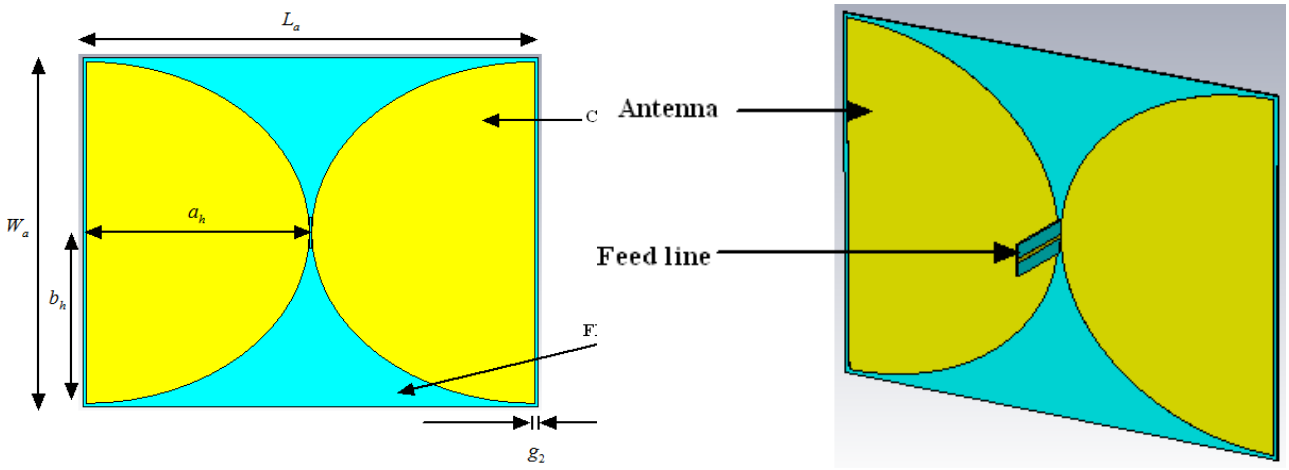

(a) Front view of the basic HEBTA (b) Perspective View of the basic HEBTA

Figure 4.8: Design of basic Half elliptical Bowtie antenna (HEBTA)

4.4.2 Stage-2: Design and Analysis of the Improved RC-loaded HEBTA

In this stage, an improved partially loaded RC-loading scheme is realized by using RF resistors, graphite sheet, EM absorbing materials and slots created on the either sides

of the Bow-tie arms. The proposed antenna will be able to attain UWB performance by the employing this improved loading scheme without compromising on the radiation efficiency.The detailed steps of this stage are discussed below.

(i) Improved Design-I: HEBTA with RF Resistor Loading

The HEBTA is loaded with four number RF resistors of 100 Ω similar to the approach as mentioned in [46]. The value of these resistors are decided by using the Wu-King (WK) resistive profile as mentioned in Equation 4.3 reported in [25, 26]. The calculated initial loading resistance value from the WK resistive profile is found to be 47 Ω which is rounded up to the nearest easily available commercial RF resistors of 50 Ω. Four number of 100 Ω are used as the loading resistors as the result is mainly dependent on total parallel loading resistances and is independent of the number of resistors [34]. The end-resistor values are also optimized by using the inbuilt optimizer of the CST Microwave studio and is also observed that there is no significant difference in the result for the change of resistance value from 47 Ω to 50 Ω. The resistors are placed at the corner positions to absorb the maximum amount of current as the current usually concentrates at the corners [34]. This type of discrete RF resistor loading helps to increase the bandwidth of the antenna by lowering the lower cutoff frequency without decreasing the radiation efficiency significantly. The resistive loaded HEBTA is as shown in Figure 4.9a.

$$R(z) = \frac{R_0}{1 + \frac{z}{H}} \tag{4.3}$$

where R_0=Resistance at the feed point in Ω, H= Antenna length (arm length length) in mm, and Z=Distance along the antenna in m.

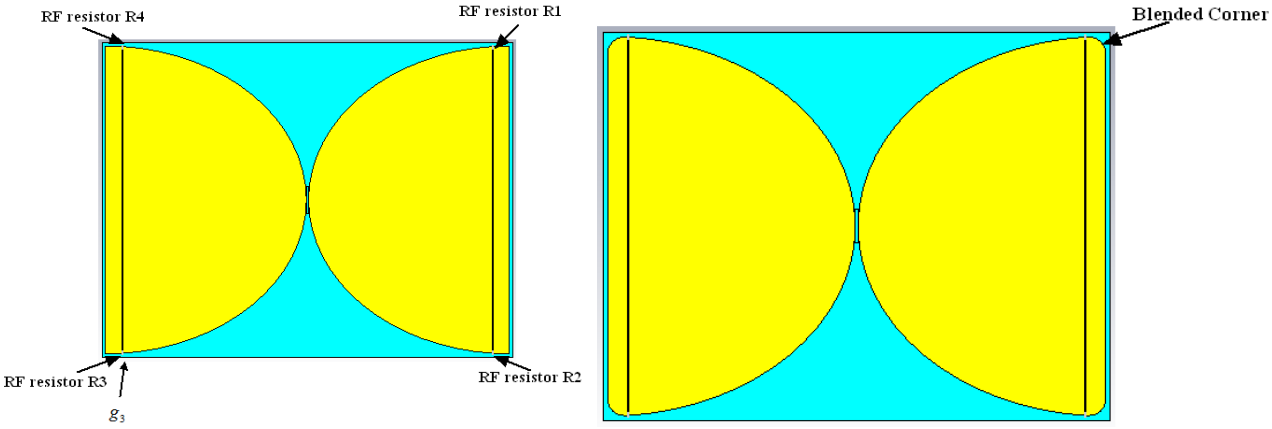

(a) Improved design-I: HEBTA loaded with RF resistors (b) Improved design-II: HEBTA with blended corners

Figure 4.9: Improved designs of HEBTA with RF resistors and blended corners

(ii) Improved Design-II: HEBTA with Blended Corners

The sharp corners of the antenna are blended so as to facilitate smooth flow of current which results in the reduction end-fire reflections and increase in radiation efficiency [51] . This help to attain the UWB performance as the input impedance of the antenna also become more smother due to these rounded corners. The radius of the curvature of the blending, i.e. r is chosen as 10 mm based on the parametric analysis carried out by the CST software. The HEBTA with blended corners is shown in Figure 4.9b.

(iii) Improved Design-III: HEBTA with RC loading

Resistive loading is most effective loading scheme to decrease late-time ringing effectively at the cost of radiation efficiency and capacitive loading still exhibits relatively high level of ringing [40]. Hence, there is the requirement of both combination of resistive loading and capacitive loading to form RC-loading scheme which will decrease the ringing to the desired level without reducing the radiation efficiency significantly. In this step, two slots having width s_1 and s_2 two provide capacitive loading at the either ends of the bow-tie antenna. The values of the w_1, w_2, w_3, s_1 and s_2 are selected to provide constant resistive and linear capacitive profile as reported in [40]. The modified expressions used for the calculation of the parameters for the capacitive loading are given in Equations 4.4 and 4.5. The RC-loaded HEBTA is shown in Figure 4.10.

$$w_n - w_{n+1} = 0.2, \quad n = 1, 2, 3 \tag{4.4}$$

$$s_{n+1} - s_n = 0.2, \quad n = 1, 2 \tag{4.5}$$

The improved designs of HEBTA with only capacitive loading and RC-loading are shown in Figure 4.10.

(iv) Improved Design-IV: HEBTA with Graphite Loading

A thin graphite sheet having conductivity of $\frac{1}{600}$ times that of copper is placed over the slot are of the Bow-tie antenna so as to further shift the lower cutoff frequency towards lower frequency range [6, 12]. The thickness of the graphite sheet, i.e. t_g is taken as 1 mm based on the parametric analysis. The HEBTA with loaded graphite sheet is shown in Figure 4.11a.

(v) Improved Design-V: HEBTA with EM Absorbing Materials

Two small pieces of the electromagnetic (EM) planar absorbing materials having height t_a is placed above the graphite sheet to further reduce the lower cut-off frequency. The conductivity of the absorbing materials are selected based on the optimistic compromise between the Atteia's work [47] as expressed in Equation 4.6 and availability of the material.

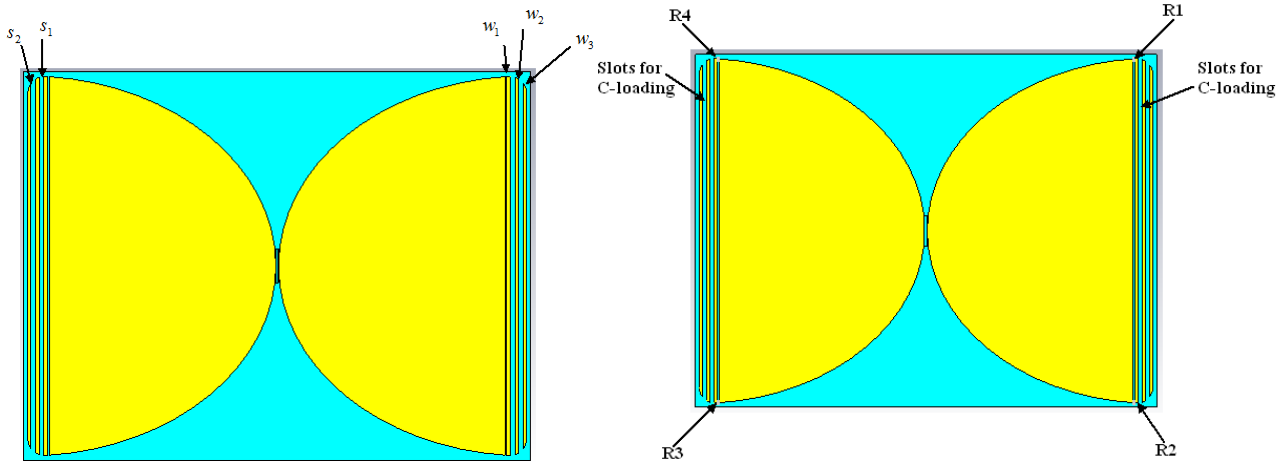

(a) HEBTA loaded with only capacitive loading (b) Improved design-III: HEBTA with RC-loading

Figure 4.10: Improved design of HEBTA with RC loading

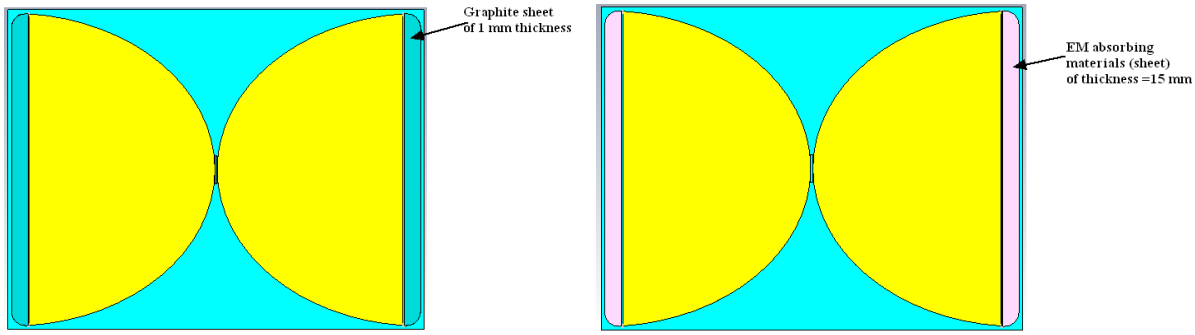

(a) Improved design-IV: HEBTA loaded with Graphite loading (b) Improved design-V: HEBTA with EM absorbing materials

Figure 4.11: Improved designs of HEBTA with Graphite loading and EM absorbing materials

The thickness of the absorbing material is selected as 15 mm based on the parametric analysis using CST Microwave studio.The improved HEBTA with EM absorbing materials is shown in Figure 4.11b.

$$\sigma = 10^{n-3} S.m^{-1}, \quad where\ n = layer\ number = 1, 2, 3... \tag{4.6}$$

4.4.3 Stage-3: Design and Analysis of the Improved RC-loaded HEBTA with Meta-material Lens

(i) Design of an improved MM Unit cell

Meta-materials (MM) are one type of artificially created media engineered to achieve either positive or negative values suitable for a particular application and performance of the MM is defined by its constitutive parameters, i.e. permittivity, permeability and refractive index, etc. Recently, the use of meta-material lens in the antenna design, has gained significant

Table 4.3: Design parameter of the unit cell in mm

l_1	1	l_4	0.2	w_3	0.2774	w_6	1	w_9	1.1938
l_2	2	w_1	3.1	w_4	0.2	w_7	1	w_{10}	0.3
l_3	10	w_2	0.6096	w_5	1	w_8	0.5	w_{11}	0.4

attention due to its focusing action. Only 1^{st} quadrant materials, i.e. double positive (DPS) materials and 3^{rd} quadrant materials, i.e. double negative (DNG) materials can be used for the lens applications due to their focusing ability [6]. Initially, an modified form of the unit cell as reported in [6, 12, 69] is designed using CST Microwave Studio v.15. The physical dimensions of the unit cell are as given in Table 4.3. The designed unit cell and the planar metamaterial lens are modified form of the unit cell reported in [6, 69] as shown in Figure 4.12. Boundary set up for the simulation of the unit cell in CST Microwave studio v.15 is shown in Figure 4.12b. The obtained S-parameters of the unit cell simulation from the simulation is presented in Figure 4.13. From this, it is observed that $|S_{21}|$ attains its minimum value at frequency of 1.12 GHz and hence it is expected that negative refractive index will available from this frequency. The other parameters such as refractive index, permeability and permittivity are extracted from the S-parameters by using the template based post processing of the CST Microwave studio [70]. The permittivity ϵ and permeability μ of the unit cell are as shown in Figure 4.14. The obtained refractive index n of the unit cell as presented in Figure 4.15 shows that the designed meta-material exhibits negative refractive index for a frequency range from 1.25 GHz to 4 GHz and positive refractive index from 0 GHz to 1.125 GHz. Hence, it is expected that gain and directivity of the designed antenna can be enhanced significantly for the frequency range of 1.125 GHz to 4 GHz significantly by using this planar metamaterial based lens.

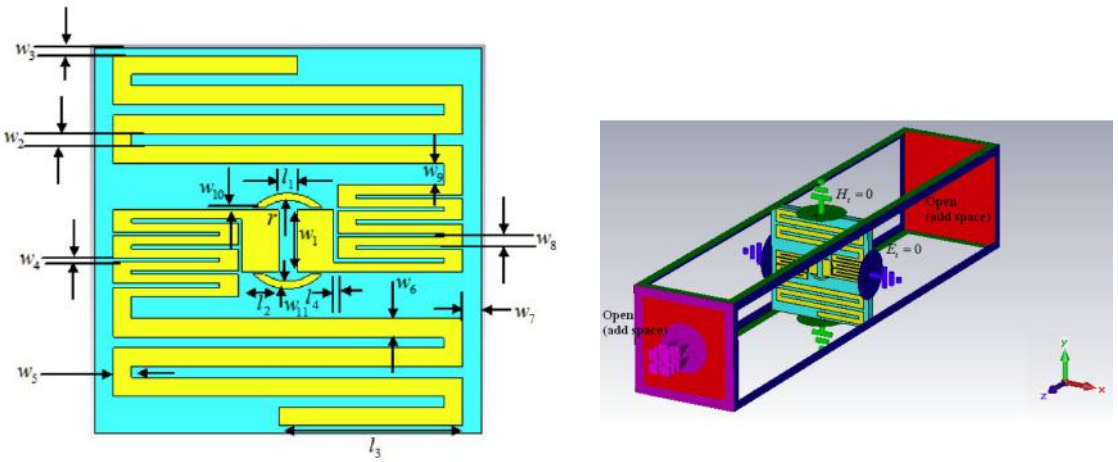

(a) The unit cell

(b) Boundary set up of the unit cell for the simulation in CST Microwave studio

Figure 4.12: Metamaterial based planar lens

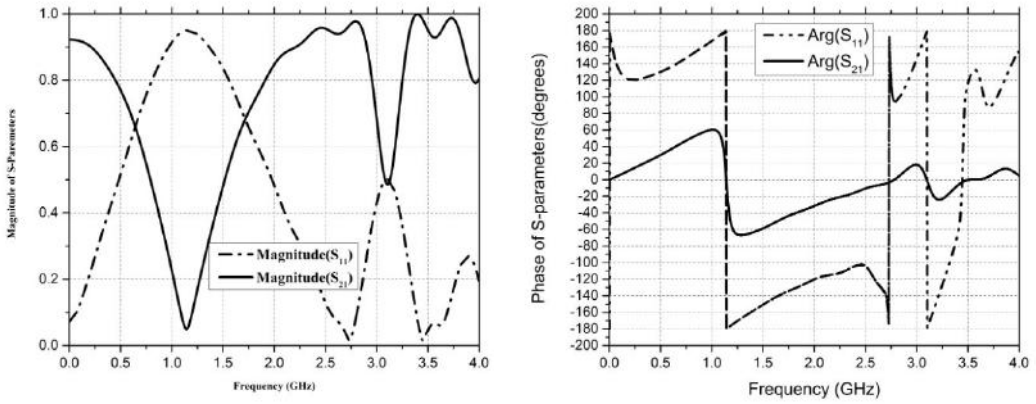

(a) Magnitude plot (b) Phase plot

Figure 4.13: S_{11} Vs Frequency plots of the unit cell

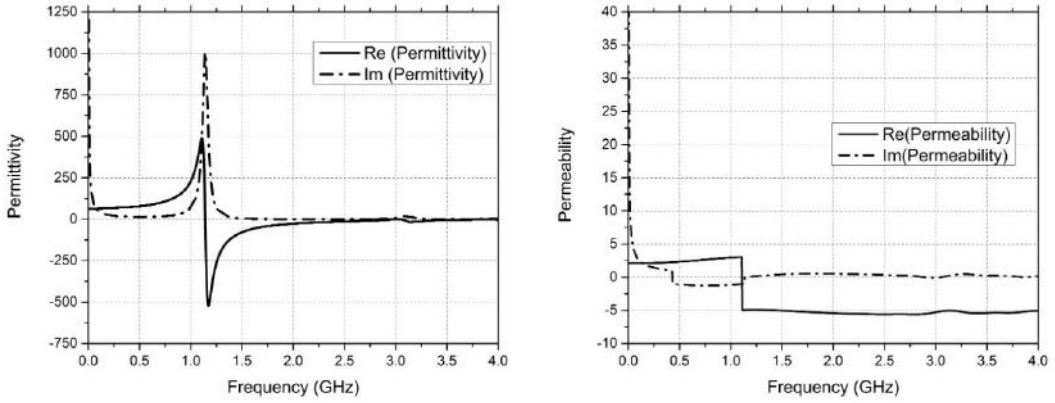

(a) Permittivity of the unit cell (b) permeability of the unit

Figure 4.14: Permittivity and permeability of the unit cell

(ii) Integration of meta-material lens to the RC-loaded HEBTA

The designed planar metamaterial based lens of 10×13 arrays of the unit cells is shown in Figure 4.16a. The designed lens is placed in front of the RC-loaded half-elliptical Bowtie antenna as shown in Figure 4.16b. The spacing h_m between the RC-loaded Bow-tie antenna and the planar lens is fixed at 14.4 mm based on the parametric analysis .The lens will act as an effective distributed inductor which will be perfectly matched to the capacitance of the bow-tie antenna to form a naturally resonant LC structure which will act as resistive source to the load [69]. Hence, the lens will enhance the overall radiation efficiency of the antenna. In other ways, it can be said that the lens will decrease the overall inductance value which in turn increase the surface resistance of the antenna.This will helps in the reduction of the surface waves of the antenna which will result in increase of the directivity and hence gain of the antenna [71]. It is also expected that to gain and directivity of the antenna will increase due to the focusing action of the MM lens and the efficiency of the antenna will also slightly

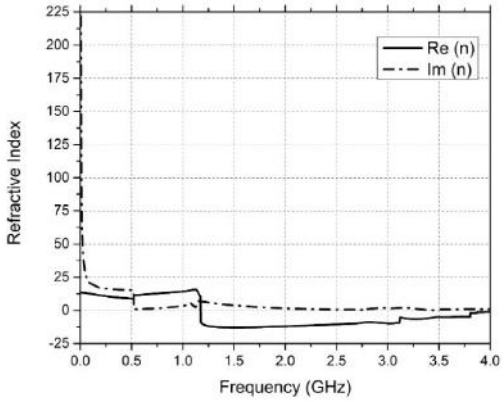

Figure 4.15: Refractive index of the unit cell

decreases due to the secondary level reflections occurring from the lens.

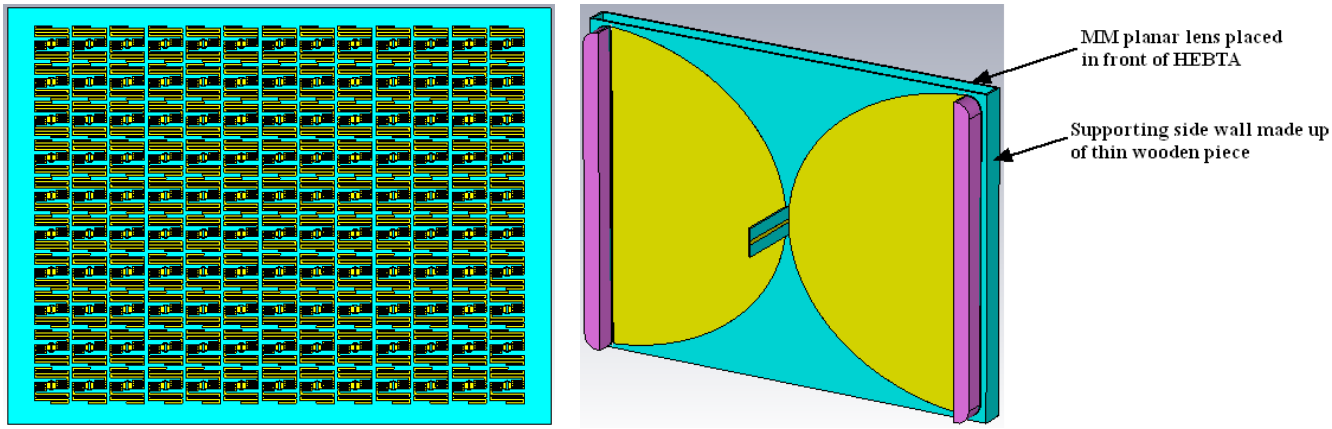

(a) Meta-material based planar lens

(b) Improved RC-loaded HEBTA with MM lens (Perspective view)

Figure 4.16: Improved design of HEBTA with RC loading

4.5 Results and Discussions

The proposed antenna is designed and simulated in CST Microwave studio v.15 installed in a PC having Intel (R) Core (TM) i7- octa core processor and 32 GB RAM. This section can be further classified into two subsections as follows.

4.5.1 Simulation Results

All the simulated results for the various antenna performance parameters are obtained through a rigorous simulations involving parametric analysis and inbuilt optimization with help of the CST Microwave Studio. These are can be briefly explained as follows.

(i) S_{11} Performance

The S_{11} performance of the basic design, improved design I, II and III of the HEBTA antenna are shown in Figure 4.17a. From this it is indicative that the lower cutoff frequency of the basic HEBTA is shifted from 0.4 GHz to 0.35 GHz due to resistive loading realized with help of four number of RF resistors. Further, lower cut-off frequency is shifted to 0.31 GHz due to implication of blended corners and RC-loading. Figure 4.17b indicated that the lower cut-off frequency is further shifted to 0.3 GHz due to the employment of graphite loading as it decreases increases the surface resistance between the copper clad and the graphite sheet.Again, from Figure 4.18a, it observed that the lower cut-off frequency is shifted to 0.29 GHz due to placement of EM absorbing materials. This signifies that the antenna is able to attain UWB performance of3.71 GHz (0.29 GHz - 4 GHz) due to the partially composite RC-loading scheme. However, from Figure 4.18 is observed that due to placement of the MM lens in front of the antenna, the minimum S_{11} label increases from -45.3 dB to -35 dB at the frequency of 0.35 GHz which signifies the reduction of the radiation efficiency due to the addition of the MM lens. It is also a point to be indicated that the higher cut-off frequency is selected at a frequency of 4 GHz though the $|S_{11}|$ level also remains below -10 dB at the frequency of 4 GHz. This is due to the fact that the higher frequencies will not penetrate sufficiently in to the soil so as to extract reflected signals from the buried targets of discontinuities due to the frequency dependent behavior of the soil [47].

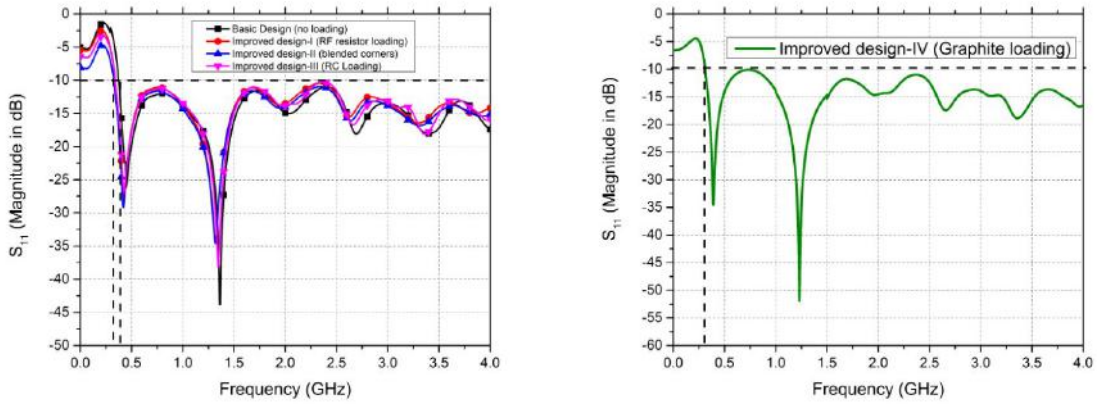

(a) S_{11} Vs Frequency plots of basic and improved designs of HEBTA

(b) S_{11} Vs Frequency plots of HEBTA with graphite loading

Figure 4.17: S_{11} performances of basic and improved designs of HEBTA

(ii) Directivity

Due to the placement of the MM lens in front of the antenna, it is observed that the directivity is improved significantly as shown in Figure 4.19a. The maximum value and minimum value of the directivity obtained through out the band is 13.1 dBi at frequency of 2 GHz and 7 dBi

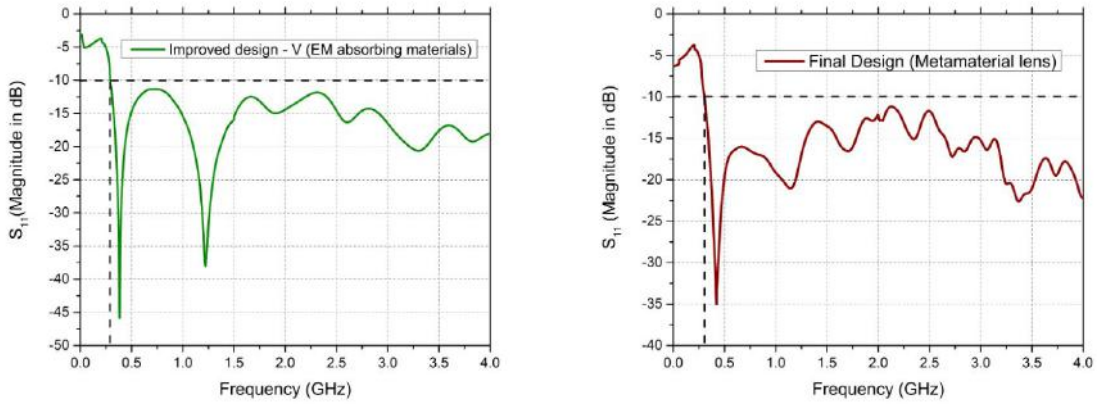

(a) S_{11} Vs Frequency plots of HEBTA with EM absorbing materials (b) S_{11} Vs Frequency plots of HEBTA with MM lens

Figure 4.18: S_{11} performances of improved and final designs of HEBTA

at frequency of 0.29 GHz respectively. This is resulted due to the focusing action of the MM lens. This high level of directivity will help the antenna to couple more energy in to the ground during the GPR applications.

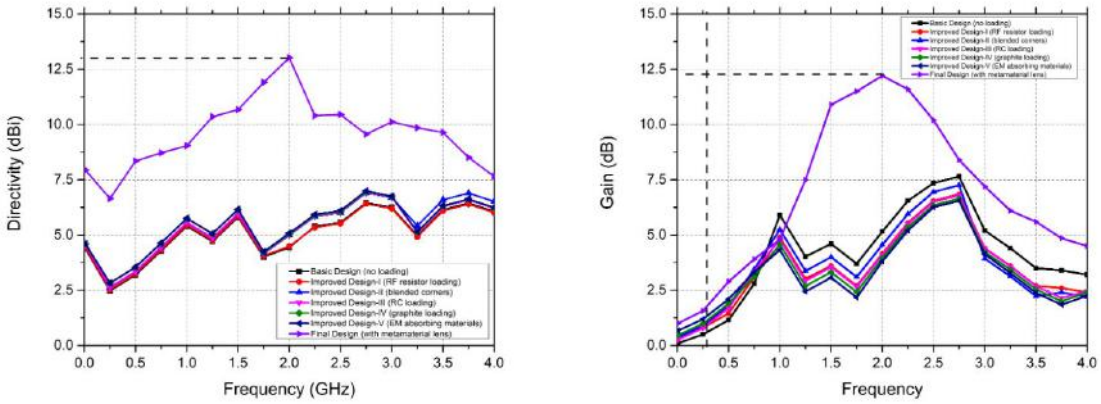

(a) Directivity Vs Frequency plots (b) Gain Vs Frequency plots

Figure 4.19: Directivity and Gain performances of RC-loaded HEBTA with MM lens

(iii) Gain

Due to the focusing action of the MM lens the directivity increases which results in the increase of the gain of the antenna. The gain Vs frequency plot of the antenna is shown in Figure 4.19b. This indicates that the maximum gain is improved from 7.5 dB to 12.4 dB due to introduction of MM lens. The maximum and minimum value of the obtained gain are 12.4 dB and 1.5 dB respectively. This increase in the gain will helps to improve the received signal amplitude during the GPR applications.

(iv) Radiation Efficiency

The radiation efficiency Vs frequency plot of the designed antenna is shown in Figure 4.20a. The UWB performance [0.29 GHz-4 GHz] of the antenna is obtained using the improved RC-loading scheme with a promising maximum and minimum radiation efficiency of 95 % and 78 %. However, the efficiency decreases significantly to a tolerable level due to addition of the MM lens. This is also acceptable as it provides significant enhancement in gain and directivity at the cost of radiation efficiency. The maximum and minimum obtained radiation efficiency of the final antenna through out the said band for the proposed antenna is 84% and 58% respectively.

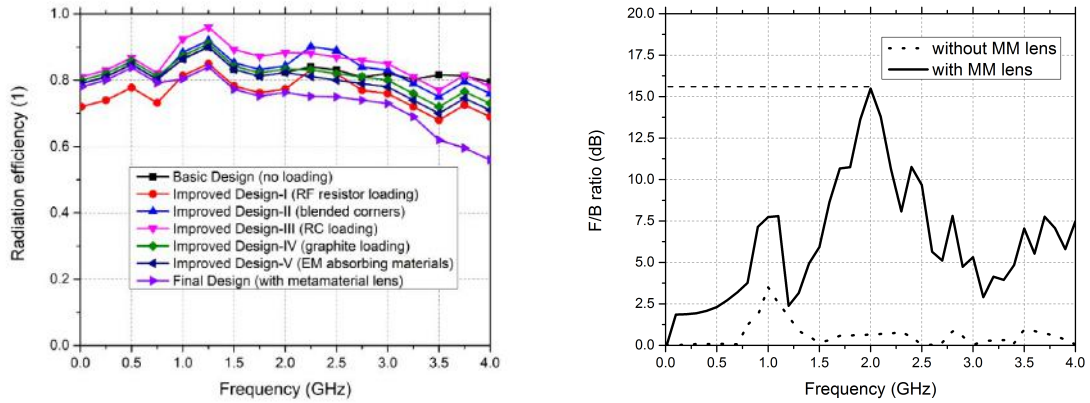

(a) Radiation efficiency Vs Frequency plots

(b) Front-to-Back ratio Vs Frequency plots

Figure 4.20: Radiation efficiency and Front-to-Back ratio performances of RC-loaded HEBTA with MM lens

(v) Front-to-Back Ratio

Front-to-back ratio can be defined as the ratio of the gain in the boresight direction to that of the backside direction [6].The proposed antenna possesses a high front-to-back F/B of 15.48 at the frequency of 2 GHz due to the MM lens. This will helps to minimize the clutter significantly during the GPR survey. The F/B Vs frequency plot of the improved RC-loaded HEBTA with MM lens is shown in Figure 4.20b.

(vi) Antenna Input Impedance

It is expected that the input impedance at the dc or zero frequency should be approximately twice of the total parallel end resistance as the resistors at the either ends are connected to each other through the directors or extended patch [34]. The magnitude of the input impedance (as input impedance is a complex quantity) of the proposed antenna is shown in the Figure 4.21. From the plot, it is indicative that the input impedance of the antenna without loading at the dc frequency is 95 Ω which is very much close to the 100 Ω, i.e. twice

of the total parallel end-resistance value of 50 Ω. It also shows that the input impedance of the HEBTA is less than that of the triangular Bow-tie antenna (optimized for 100 Ω) due to the non-linear flaring nature of the elliptical structure.

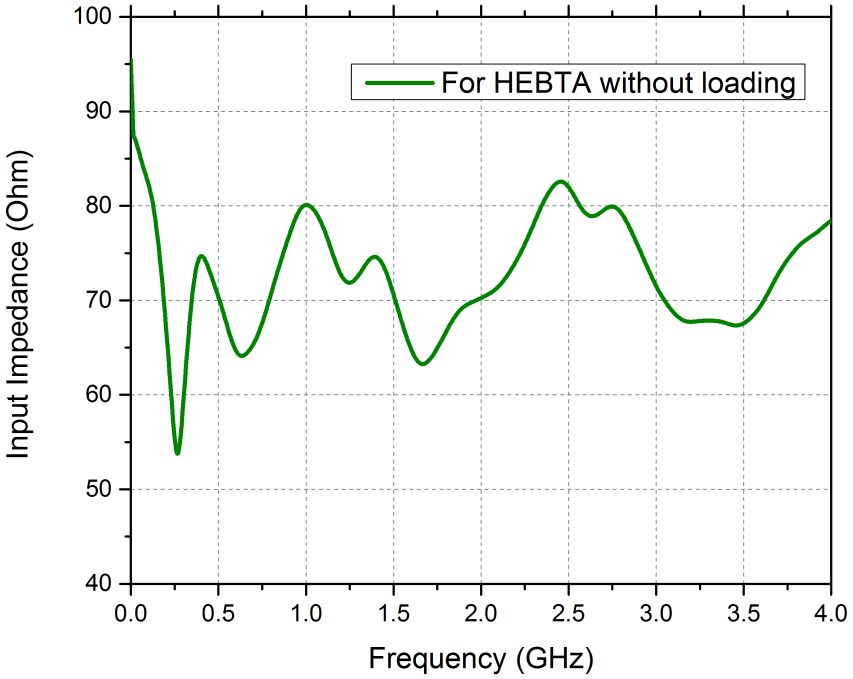

Figure 4.21: Input impedance of the HEBTA

(vii) Far Field Radiation Patterns

The polar plots of the far-field radiation patterns of the proposed antenna for the worst case scenario are shown in Figure 4.22. The E-plane pattern is obtained at ϕ= 100^0 and H-plane pattern is obtained at θ=10^0. Comprehensive results of the radiation pattern for the whole said band is as given in Table 4.4. From the table it is also indicative that the beam width gradually increases in the higher frequency range. However, it will not be a problem for the GPR applications as the high frequency signal will not penetrate sufficiently.

4.5.2 Discussions

The antenna is also simulated using HFSS v.15 by using the HPC (high performance computing) cluster with 32 computing nodes (Intel Xeon 2.0 GHz, two CPU 16 cores, 64GB) facility available in the institute. The result obtained from HFSS are compared with the results obtained from the CST. Figure 4.23a shows that the return loss performance obtained from both the tools are agree to high level. Further, it is also indicative from the Figure 4.23b that radiation efficiencies obtained from both tools matches closely. The directivity and gain

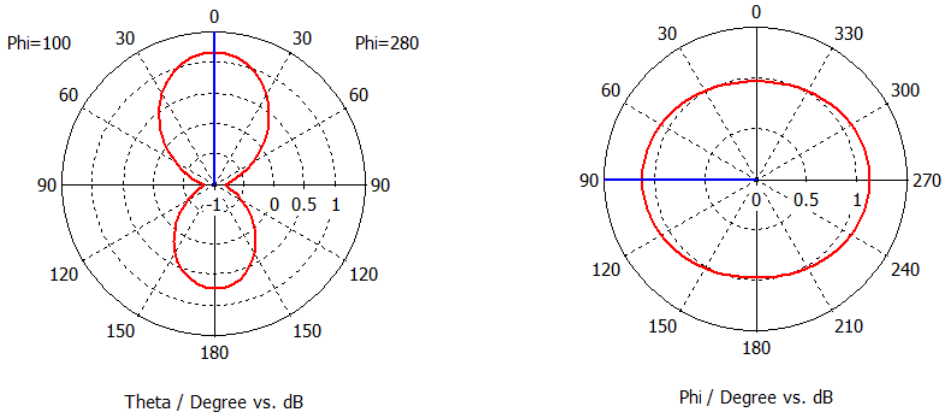

(a) E-plane pattern (b) H-plane pattern

Figure 4.22: Far field radiation patterns at f= 0.3 GHz

Table 4.4: Farfield Results of the Proposed RC-loaded HEBTA with MM lens

Frequency (GHz)	E-plane		H-plane	
	Main lobe magnitude (dB)	Angular 3dB Beam width (degree)	Main lobe magnitude (dB)	Angular 3dB Beam width (degree)
0.3	1.17	35.5	1.12	31.37
0.5	2.88	45.15	2.79	46.35
1	4.78	47.15	4.65	46.72
1.5	10.9	41.20	9.89	40.15
2	12.15	30.25	11.85	33.20
2.5	10.19	33.4	10.15	34.25
3	7.18	39.5	7.08	37.6
3.5	5.59	45.6	5.21	44.8
4	4.48	50.7	4.40	52.8

of the antenna obtained from both the tools shows a high degree of correlation as shown in Figure 4.24. Both CST and HFSS are based on two different numerical techniques, i.e. finite integration technique (FIT) and finite element method (FEM) respectively. Hence, the high degree of similarity between the results obtained from both the tools provides enough confidence that the fabricated antenna will provide the results very close to the simulated ones.

4.6 Simulation of the Proposed Antenna with Thermal and Mechanical solvers

To study the impact of temperature variations on the antenna performances, the antenna is simulated using Multi-physics solvers of the CST Microwave studio v.15. From Figure 4.25 it is observed that the overall antenna performance is affected little bit. Hence, it indicated

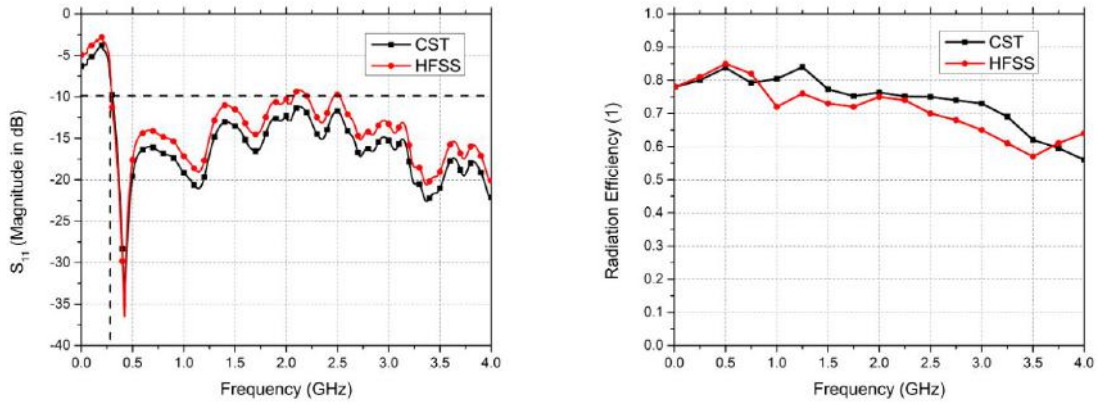

(a) Comparison of S_{11} performances

(b) Comparison of radiation efficiencies

Figure 4.23: Comparison of S_{11} and radiation efficiencies obtained from CST and HFSS

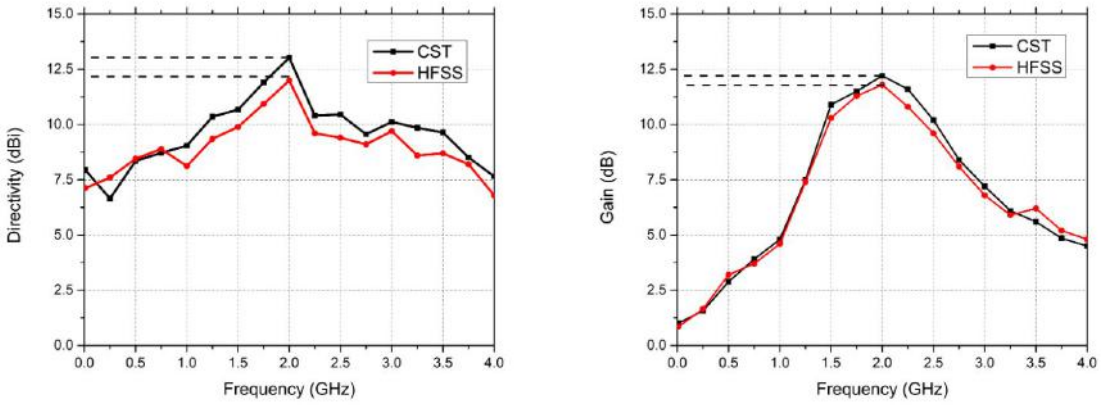

(a) Comparison of directivity

(b) Comparison of gain

Figure 4.24: Comparison of directivity and gain obtained from CST and HFSS

that the designed antenna is not prone to the temperature variation.

4.7 Performance Evaluation of the Antenna in the GPR Scenario using CST MW studio

The proposed antenna is simulated in GPR scenario implemented in CST Microwave studio to investigate the antenna performance in the GPR scenario as shown in Figure 4.26a. For simplicity, the host media is taken as a layered media consists of three different layers. The first layer is dry sandy soil ($\varepsilon_r = 2.53, \mu = 1, \sigma = 0.0036$) of thickness 15 mm, second layer is wet sandy soil ($\varepsilon_r = 13, \mu = 1, \sigma = 0.029$) of thickness 20 mm and the third layer is wet loamy soil ($\varepsilon_r = 13.80, \mu = 1, \sigma = 0.18$) which is infinite in thickness. The S_{11} performance of the antenna in the ideal environment (in air medium) is compared with that

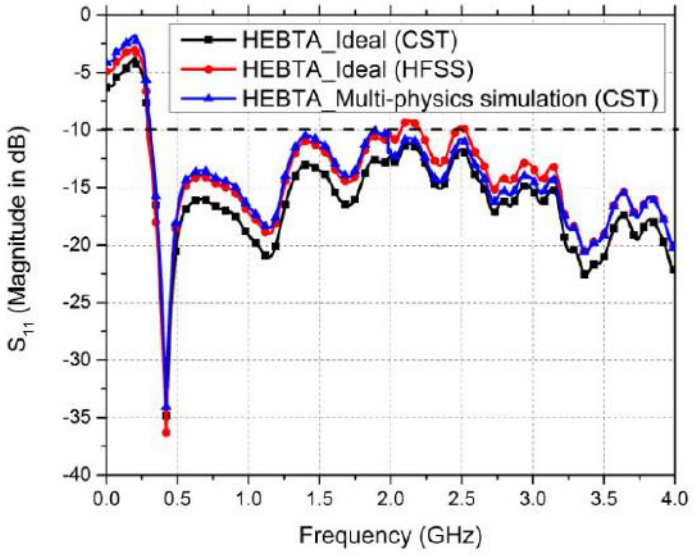

Figure 4.25: Thermal and Mechanical Co-simulation of the Antenna

of in the GPR scenario as shown in Figure 4.26b. It is observed that the antenna performance differs significantly in the GPR scenario from that of ideal case. Hence, the GPR antenna should be designed for the particular application corresponding to the nature of the host media and desired range and resolution of the GPR system.

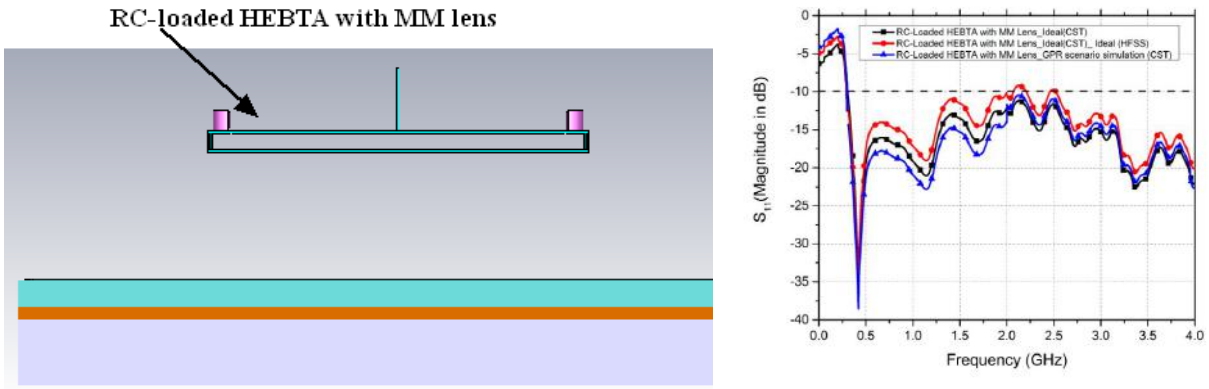

(a) Simulation of the antenna in GPR scenario implemented in CST (b) Comparison of S_{11} performances

Figure 4.26: Performance Evaluation of the Antenna in the GPR Scenario using CST

4.8 Comparative Analysis of the Proposed Antenna with other Existing Antennas

As the antenna could not be fabricated for the timing, the simulated results of the proposed antenna are compared with the that of the other Bow-tie antennas for GPR applications

reported in the literature as shown in Table 4.5. From this comparative analysis, it observed that our proposed antennas provide a promising results with respect to gain, radiation efficiency and front-to-back ratio. Our antennas are also compact and lightweight in nature which increases its potential for the GPR applications.

Table 4.5: Comparative analysis of the antenna with other reported antennas for the GPR applications

Ref:	Antenna Type	Frequency & operation		Gain in the operating band		Radiation Efficiency		Max F/B ratio	Size
		f_{min} (GHz)	f_{max} (GHz)	G_{min} (dB)	G_{max} (dB)	η_{min} (%)	η_{max} (%)		
[40]	RC-loaded	0.5	5	Not Known	Not Known	Not Known	Not Known	Not Known	50 cm
[26]	Resistive loaded vee dipole	0.5	8	6.6	-20	Not Known	Not Known	Not Known	17.15*11.43 cm^2
[46]	Cavity backed resistive loaded half ellipse	0.25	0.75	Not Known	Not Known	Not Known	Not Known	Not Known	30*18 cm^2
[6, 12]	Bow-tie with MM lens	0.3	3	11.52	-10	0.44	90	15.39	30*23 cm^2
[48]	CPW fed cavity backed Bow-tie antenna	0.4	1.5	Not Known	Not Known	Not Known	Not Known	Not Known	50.3*22 cm^2
[47]	Cavity backed slot antenna	0.46	4	-6	4.2	Not Known	Not Known	Not Known	36*23 cm^2
[30]	Resistive loaded Bow-tie	0.5	5	Not Known	Not Known	Not Known	Not Known	Not Known	23*7 cm^2
[72]	wire Bow-tie	0.5	5	Not Known	Not Known	Not Known	Not Known	Not Known	50 cm
[73] Proposed Antenna-1	CPW fed resistive loaded slot Bow-tie	0.4	4.5	7	2.8	60	80.5	0	51*22 cm^2
Proposed Antenna-2	RC-loaded HEBTA with MM lens	0.29	4	1.5	12.4	58	94	15.48	30*23 cm^2

4.9 Summary

An improved partially covered RC-loaded half-elliptical bow-tie antenna having impedance bandwidth 172 % (0.29 GHz- 4 GHz) is proposed. The proposed improved RC-loading scheme is able to provide UWB performance without decreasing the radiation efficiency significantly. It is also capable of providing maximum gain of 12.4 dB and minimum gain of 1.5 dB throughout the said band. The gain and directivity of the antenna is significantly increased by using the improved MM planar lens. The major limitation of this work is slightly degradation of radiation efficiency due to the use of MM lens. However, this can be prevented significantly by placing the lens at a proper distance from the antenna face. The future work should be focused on the fabrication and testing of the designed antenna in GPR scenario.

Chapter 5

Conclusion

The overall conclusion of this thesis can be briefly outlined under following two sections.

5.1 Contribution

The major contributions of this thesis work can be briefly presented as follows.

In this research work, two improved Bow-tie antennas for GPR applications are designed and investigated. The first antenna, i.e. resistive loaded Bow-tie antenna with UWB performance over 4.1 GHz frequency range (0.4GHz – 4.5 GHz) is designed to minimize the end-fire reflection by blending the sharp corners. The compactness is achieved with help of thin graphite sheet instead of volumetric EM absorbing material. However, due to only resistive loading, the radiation efficiency of the antenna decreases significantly.

To overcome this problem, we have deigned and investigated another half-elliptical Bow-tie antenna capable of operating from 0.29 GHz to 4 GHz with a maximum gain of 12.4 dB and minimum gain of 1.5 dB throughout the band. Here, the improved RC-loading scheme is proposed to increase the bandwidth of the Bow-tie antenna by lowering the lower cutoff frequency without decreasing the radiation efficiency significantly. This loading scheme realized covering the Bow-tie antenna partially with the help of four numbers of discrete RF resistors, two small thin sheets of graphite and small size EM absorbing materials. A planar meta-material lens as proposed in [6] is modified to increase the operating frequency range. This is achieved with the introduction of two circular arcs around the central portion of the unit cell so as to increase the operational bandwidth without increasing the overall area of the unit cell. Hence, the overall antenna performances, i.e. gain, directivity, etc. are increased to a good level by using the improved meta-material based planar lens.

The performance of both the antennas in GPR scenario is investigated at the simulation level and is found that the design of the GPR antenna should be application specific so as to obtain the best result. As GPR system has to be operated in varieties of the odd weather or atmospheric conditions and hence, the thermal and mechanical behavior of the antennas are investigated with the help of Multi-physics simulation of CST Microwave studio V.15.

It is also observed that the designed antennas are not prone to temperature and mechanical variations.

The comparative analysis of both the designed antennas with the other reported antennas show that the obtained antenna performances such as gain, directivity, bandwidth, frequency of operation, compactness, radiation efficiency, etc. are promising and hence the designed antennas have a great potential for the GPR applications.

5.2 Future Scope

The work is carried with some constraints which can be taken as the future work of this thesis. The antennas have to be measured in the anechoic chamber so as to record its radiation patterns in free space condition. In future, both the antennas will be used in practical GPR testing to investigate the antenna performance at ground level. The loading profile can be further improved so as to obtain more efficiency. The meta-material based planar lens can be investigated to shift its DNG property towards to low-frequency range (from 1.2 GHz towards the dc value) so that significant gain and directivity can be obtained for the low-frequency operation. The antenna can be modified to achieve further compactness and high efficiency. A compact EM shielding may be designed so as to prevent the picking of the other available wireless signals such as GSM signal, Wi-Fi signal, etc. This research work may be extended to achieve the frequency reconfigurability over a wide bandwidth by these antennas with suitable structural modifications so that a single antenna can be used for multiple GPR applications.

References

[1] "Commerical gpr products by bchazmat management ltd, canada." [Online]. Available: http://bchazmat.com/bchazmat-services/ground-penetrating-radar-gpr/

[2] H. M. Jol, *Ground penetrating Radar: Theory and Applications*. elsevier, 2008.

[3] M. El-Hadidy, "State of the art of em simulation technology in communication engineering, tutorial talk, cst-middle east, egypt," *MMM'14 : 14th Mediterranean Microwave Symposium IEEE Conference, https://www.youtube.com/watch?v=GrMY0ik5uPo*, December 12-14, 2014.

[4] I. Hertl and M. Strycek, "Uwb antennas for ground penetrating radar application," *19th International Conference on Applied Electromagnetics and Communications, ICECom 2007.*, pp. 1–4, Sept 2007.

[5] A. S. Turk, D. A. Sahinkaya, M. Sezgin, and H. Nazli, "Investigation of convenient antenna designs for ultra-wide band gpr systems," *4th International Workshop on Advanced Ground Penetrating Radar*, pp. 192–196, June 2007.

[6] K. K. Ajith and A. Bhattacharya, "Printed compact lens antenna for uhf band applications," *Progress In Electromagnetics Research C*, vol. 62, pp. 11–22, 2016.

[7] D. J. Daniels, *Ground penetrating radar*. The Institute of Electrical Engineers, London, 2004.

[8] R. Persico, *Introduction to ground penetrating radar: inverse scattering and data processing*. John Wiley & Sons, 2014.

[9] B. Scheers, "Ultra-wideband ground penetrating radar, with application to the detection of anti personnel landmines," Ph.D. dissertation, TU Delft, 2001.

[10] S. Lambot, T. Mishra, and A. Bhattacharya, "Geological exploration by ground penetrating radar," *Course materails of the International summer and winter course term, IIT Kharagpur*, May 2014.

[11] W. Wiesbeck, G. Adamiuk, and C. Sturm, "Basic properties and design principles of uwb antennas," *Proceedings of the IEEE*, vol. 97, no. 2, pp. 372–385, Feb 2009.

[12] K. K. Ajith and A. Bhattacharya, "Improved ultra-wide bandwidth bow-tie antenna with metamaterial lens for gpr applications," *15th International Conference on Ground Penetrating Radar (GPR)*, pp. 739–744, June 2014.

[13] Y. Tao, S. Kan, and G. Wang, "Ultra-wideband bow-tie antenna design," *IEEE International Conference on Ultra-Wideband*, vol. 1, pp. 1–3, Sept 2010.

[14] S. Millard, A. Shaari, and J. Bungey, "Field pattern characteristics of gpr antennas," *NDT & E International*, vol. 35, no. 7, pp. 473–482, 2002.

[15] G. Quintero, J. F. Zurcher, and A. K. Skrivervik, "System fidelity factor: A new method for comparing uwb antennas," *IEEE Transactions on Antennas and Propagation*, vol. 59, no. 7, pp. 2502–2512, July 2011.

[16] Y. Duroc, A. Ghiotto, T. P. Vuong, and S. Tedjini, "Uwb antennas: Systems with transfer function and impulse response," *IEEE Transactions on Antennas and Propagation*, vol. 55, no. 5, pp. 1449–1451, May 2007.

[17] Y. Duroc, A. I. Najam, T. P. Vuong, and S. Tedjini, "Modeling and state representation of ultrawideband antennas," *IEEE Transactions on Antennas and Propagation*, vol. 57, no. 9, pp. 2781–2784, Sept 2009.

[18] X. Li, S. C. Hagness, M. K. Choi, and D. W. van der Weide, "Numerical and experimental investigation of an ultrawideband ridged pyramidal horn antenna with curved launching plane for pulse radiation," *IEEE Antennas and Wireless Propagation Letters*, vol. 2, no. 1, pp. 259–262, 2003.

[19] J. Wang, Y. Su, C. Huang, M. Lu, and Y. Li, "Design of bow-tie antenna with high radiating efficiency for impulse gpr," *IEEE International Geoscience and Remote Sensing Symposium*, pp. 594–597, July 2012.

[20] K. H. Sayidmarie and Y. A. Fadhel, "A planar self-complementary bow-tie antenna for uwb applications," *Progress In Electromagnetics Research C*, vol. 35, pp. 253–267, 2013.

[21] G. Wang, J. Liu, J. Xia, and L. Yang, "Coaxial-fed double-sided bow-tie antenna for gsm/cdma and 3g/wlan communications," *IEEE Transactions on Antennas and Propagation*, vol. 56, no. 8, pp. 2739–2742, Aug 2008.

[22] H. Wang, J. Liu, and G. Wang, "Asymmetric bow-tie antenna for gsm/cdma and 3g/wlan," *Electronics Letters*, vol. 43, no. 23, Nov 2007.

[23] A. A. Eldek, A. Z. Elsherbeni, and C. E. Smith, "Characteristics of bow-tie slot antenna with tapered tuning stubs for wideband operation," *Progress In Electromagnetics Research*, vol. 49, pp. 53–69, 2004.

[24] D. Caratelli and A. Yarovoy, "Design and full-wave analysis of cavity-backed bow-tie antennas for low-frequency gpr applications," *13th International Conference on Ground Penetrating Radar (GPR)*, pp. 1–10, June 2010.

[25] J. G. Maloney and G. S. Smith, "A study of transient radiation from the wu-king resistive monopole-fdtd analysis and experimental measurements," *IEEE Transactions on Antennas and Propagation*, vol. 41, no. 5, pp. 668–676, May 1993.

[26] K. Kim and W. R. Scott, "Design of a resistively loaded vee dipole for ultrawide-band ground-penetrating radar applications," *IEEE Transactions on Antennas and Propagation*, vol. 53, no. 8, pp. 2525–2532, Aug 2005.

[27] E. S. Eide, "Ultra-wideband transmit/receive antenna pair for ground penetrating radar," *IEE Proceedings - Microwaves, Antennas and Propagation*, vol. 147, no. 3, pp. 231–235, Jun 2000.

[28] A. A. Lestari, Y. A. Kirana, A. B. Suksmono, A. Kurniawan, E. Bharata, A. G. Yarovo, and L. P. Ligthart, "Compact uwb radiator for short-range gpr applications," *Proceedings of the Tenth International Conference on Ground Penetrating Radar, GPR*, vol. 1, pp. 141–144, June 2004.

[29] A. A. Lestari, D. Yulian, Liarto, A. B. Suksmono, E. Bharata, A. G. Yarovoy, and L. P. Ligthart, "Improved bow-tie antenna for pulse radiation and its implementation in a gpr survey," *4th International Workshop on Advanced Ground Penetrating Radar*, pp. 197–202, June 2007.

[30] A. A. Lestari, E. Bharata, A. B. Suksmono, A. Kurniawan, A. G. Yarovoy, and L. P. Ligthart, "A modified bow-tie antenna for improved pulse radiation," *IEEE Transactions on Antennas and Propagation*, vol. 58, no. 7, pp. 2184–2192, July 2010.

[31] Y. Guo, L. Xu, and X. Shi, "Improved resistive loading profile for ground-penetrating radar antenna applications," *International Conference on Radar (CIE)*, pp. 543–546, Oct 2006.

[32] C. H. See, R. A. Abd-Alhameed, S. W. J. Chung, D. Zhou, H. Al-Ahmad, and P. S. Excell, "The design of a resistively loaded bowtie antenna for applications in breast cancer detection systems," *IEEE Transactions on Antennas and Propagation*, vol. 60, no. 5, pp. 2526–2530, May 2012.

[33] Y. Nishioka, O. Maeshima, T. Uno, and S. Adachi, "Fdtd analysis of resistor-loaded bow-tie antennas covered with ferrite-coated conducting cavity for subsurface radar," *IEEE Transactions on Antennas and Propagation*, vol. 47, no. 6, pp. 970–977, Jun 1999.

[34] D. Uduwawala, M. Norgren, P. Fuks, and A. W. Gunawardena, "A deep parametric study of resistor-loaded bow-tie antennas for ground-penetrating radar applications using fdtd," *IEEE Transactions on Geoscience and Remote Sensing*, vol. 42, no. 4, pp. 732–742, April 2004.

[35] A. G. Yarovoy and R. Pugliese, "Capacitevely loaded bowtie antenna for ultrawideband impulse radio," *Radio science*, vol. 41, no. 3, 2006.

[36] A. G. Yarovoy, Y. Erbas, and L. P. Ligthart, "Adaptive bow-tie antenna with increased bandwidth," *32nd European Microwave Conference*, pp. 1–4, Sept 2002.

[37] D. S. Paunovic and B. D. Popovic, "Broadband rc-loaded microwave cylindrical antenna with approximately real input admittance," *Radio and Electronic Engineer*, vol. 47, no. 5, pp. 225–228, May 1977.

[38] A. A. Lestari, A. G. Yarovoy, and L. P. Ligthart, "Analysis of rc loading profiles for antenna bandwidth improvement," *Antennas and Propagation Society International Symposium, IEEE*, vol. 3, pp. 632–635, June 2003.

[39] ——, "An efficient ultra-wideband bow-tie antenna," *31st European Microwave Conference*, pp. 1–4, Sept 2001.

[40] ——, "Rc-loaded bow-tie antenna for improved pulse radiation," *IEEE Transactions on Antennas and Propagation*, vol. 52, no. 10, pp. 2555–2563, Oct 2004.

[41] A. Zou, J. Li, K. Wang, and D. Cheng, "Investigations of rl-loaded bowtie antenna for low-resolution gpr," *5th International Conference on Wireless Communications, Networking and Mobile Computing*, pp. 1–3, Sept 2009.

[42] K. H. Lee, C. C. Chen, F. L. Teixeira, and R. Lee, "Modeling and investigation of a geometrically complex uwb gpr antenna using fdtd," *IEEE Transactions on Antennas and Propagation*, vol. 52, no. 8, pp. 1983–1991, Aug 2004.

[43] G. Chen and R. C. Liu, "A 900mhz shielded bow-tie antenna system for ground penetrating radar," *13th International Conference on Ground Penetrating Radar (GPR)*, pp. 1–6, June 2010.

[44] J. Shao, Z. Xia, Y. Ji, G. Fang, and H. Yin, "An ultra-wideband antenna for the reinforced concrete detection," *Journal of Electronics (China)*, vol. 30, no. 6, pp. 547–552, 2013.

[45] F. Congedo, G. Monti, and L. Tarricone, "Modified bowtie antenna for gpr applications," *13th International Conference on Ground Penetrating Radar (GPR)*, pp. 1–5, June 2010.

[46] B. Wu, Y. Ji, and G. Fang, "Analysis of gpr uwb half-ellipse antennas with different heights of backed cavity above ground," *IEEE Antennas and Wireless Propagation Letters*, vol. 9, pp. 130–133, 2010.

[47] F. Sagnard, "Design of a compact ultra-wide band bow-tie slot antenna system for the evaluation of structural changes in civil engineering works," *Progress In Electromagnetics Research B*, vol. 58, pp. 181–191, 2014.

[48] F. Sagnard and F. Rejiba, "Wide band coplanar waveguide-fed bowtie slot antenna for a large range of ground penetrating radar applications," *IET Microwaves, Antennas Propagation*, vol. 5, no. 6, pp. 734–739, April 2011.

[49] M. Midrio, S. Boscolo, F. Sacchetto, M. Pascolini, F. M. Pigozzo, and A. D. Capobianco, "A novel uwb bow-tie antenna design with high f/b ratio and directivity," *38th European Microwave Conference (EuMC 2008)*, pp. 393–396, Oct 2008.

[50] D. Yang, J. Pan, Z. Zhao, and Z. Nie, "Design of trapezoidal cavity-backed resistance loaded bow tie antenna with ultra-wideband and high directivity," *Journal of Electromagnetic Waves and Applications*, vol. 24, no. 11-12, pp. 1685–1695, 2010.

[51] S.-W. Qu and C.-L. Ruan, "Effect of round corners on bowtie antennas," *Progress In Electromagnetics Research*, vol. 57, pp. 179–195, 2006.

[52] A. C. Durgun, C. A. Balanis, C. R. Birtcher, and D. R. Allee, "Design, simulation, fabrication and testing of flexible bow-tie antennas," *IEEE Transactions on Antennas and Propagation*, vol. 59, no. 12, pp. 4425–4435, Dec 2011.

[53] J.-Y. Zhao, Z.-Y. Zhang, N.-W. Liu, G. Fu, and S.-X. Gong, "Wideband unidirectional bowtie antenna with pattern improvement," *Progress In Electromagnetics Research Letters*, vol. 44, pp. 119–124, 2014.

[54] Q. Xue, S.-W. Qu, and C. H. Chan, "Wideband cavity-backed bowtie antennas," *IEEE International Workshop on Antenna Technology (iWAT)*, pp. 1–4, March 2009.

[55] S. W. Qu, J. L. Li, Q. Xue, C. H. Chan, and S. Li, "Wideband and unidirectional cavity-backed folded triangular bowtie antenna," *IEEE Transactions on Antennas and Propagation*, vol. 57, no. 4, pp. 1259–1263, April 2009.

[56] S.-W. Qu, C. H. Chan, and Q. Xue, "Ultrawideband composite cavity-backed rounded triangular bowtie antenna with stable patterns," *Journal of Electromagnetic Waves and Applications*, vol. 23, no. 5-6, pp. 685–695, 2009.

[57] R. Persico and G. Prisco, "A reconfigurative approach for sf-gpr prospecting," *IEEE Transactions on Antennas and Propagation*, vol. 56, no. 8, pp. 2673–2680, Aug 2008.

[58] N. Romano, G. Prisco, and F. Soldovieri, "Design of a reconfigurable antenna for ground penetrating radar applications," *Progress In Electromagnetics Research*, vol. 94, pp. 1–18, 2009.

[59] M. K. A. Rahim, M. Z. A. A. Aziz, and C. S. Goh, "Bow-tie microstrip antenna design," *13th IEEE International Conference on Networks Jointly held with the IEEE 7th Malaysia International Conf on Communic*, vol. 1, pp. 17–20, 2005.

[60] H. J. Visser, *Antenna theory and applications*. John Wiley & Sons, 2012.

[61] R. DuHamel and D. Isbell, "Broadband logarithmically periodic antenna structures," *IRE International Convention Record*, vol. 5, pp. 119–128, March 1957.

[62] R. Carrel, "The characteristic impedance of two infinite cones of arbitrary cross section," *IRE Transactions on Antennas and Propagation*, vol. 6, no. 2, pp. 197–201, April 1958.

[63] J. Thaysen, K. B. Jakobsen, and J. Appel-Hansen, "A wideband balun-how does it work?" *Applied Microwave and Wireless*, vol. 12, no. 10, pp. 40–51, 2000.

[64] K. Vinayagamoorthy, "Design and implementation of wideband baluns for archimedean spiral antennas," *A thesis for Master of Engineering, Queensland University of Technology*, 2011.

[65] C. A. Balanis, *Antenna theory: analysis and design*. John Wiley & Sons, 2013.

[66] H. Su, "Investigations of rc-loaded bow-tie antennas for impulse ground penetrating radar applications," Ph.D. dissertation, University of Manitoba, 2006.

[67] S.-G. Kim and K. Chang, "Ultrawide-band transitions and new microwave components using double-sided parallel-strip lines," *Microwave Theory and Techniques, IEEE Transactions on*, vol. 52, no. 9, pp. 2148–2152, 2004.

[68] R. Garg, I. Bahl, and M. Bozzi, *Microstrip lines and slotlines*. Artech house, 2013.

[69] A. Erentok, R. W. Ziolkowski, J. Nielsen, R. Greegor, C. Parazzoli, M. Tanielian, S. A. Cummer, B.-I. Popa, T. Hand, D. Vier *et al.*, "Lumped element-based, highly sub-wavelength, negative index metamaterials at uhf frequencies," *Journal of Applied Physics*, vol. 104, no. 3, p. 034901, 2008.

[70] D. Smith, D. Vier, T. Koschny, and C. Soukoulis, "Electromagnetic parameter retrieval from inhomogeneous metamaterials," *Physical Review E*, vol. 71, no. 3, p. 036617, 2005.

[71] M. A. Antoniades and G. V. Eleftheriades, "Negative-refractive-index transmission-line metamaterial-loaded dipole antennas," *IEEE-APS Topical Conference on Antennas and Propagation in Wireless Communications (APWC)*, pp. 174–177, Sept 2012.

[72] A. A. Lestari, A. G. Yarovoy, and L. P. Ligthart, "Adaptive wire bow-tie antenna for ground penetrating radar," *IEEE International Proceedings on Geoscience and Remote Sensing Symposium (IGARSS 2005)*, vol. 1, pp. 368–371, July 2005.

[73] R. Nayak, S. Maiti, and S. K. Patra, "Design and simulation of compact uwb bow-tie antenna with reduced end-fire reflections for gpr applications," *IEEE International Conference on Wireless Communications Signal Processing and Networking (WiSPNET), Chennai, 23-28 March, 2016*, pp. 1835–1839, 2016.

Dissemination

[1]

1. Nayak, R., Maiti, S., & Patra, S. K., “Design and Simulation of Compact UWB Bow-tie Antenna with Reduced End-fire Reflections for GPR Applications”, IEEE International Conference WiSPNET 2016, Chennai, 24-26 March, 2016.

[1] Articles already published

Index